ISTANBUL TECHNICAL UNIVERSITY ★ GRADUATE SCHOOL OF SCIENCE
ENGINEERING AND TECHNOLOGY

SIMULATION OF FOUR ANODE PHOTOMULTIPLIERS FOR THE CMS FORWARD HADRON CALORIMETER

M.Sc. THESIS

Mete YÜCEL

Department of Physics Engineering

Physics Engineering Programme

MAY 2012

ISTANBUL TECHNICAL UNIVERSITY ★ GRADUATE SCHOOL OF SCIENCE ENGINEERING AND TECHNOLOGY

SIMULATION OF FOUR ANODE PHOTOMULTIPLIERS FOR THE CMS FORWARD HADRON CALORIMETER

M.Sc. THESIS

Mete YÜCEL
(509101131)

Department of Physics Engineering

Physics Engineering Programme

Thesis Advisor: Assoc. Prof. Dr. Kerem CANKOÇAK

MAY 2012

İSTANBUL TEKNİK ÜNİVERSİTESİ ★ FEN BİLİMLERİ ENSTİTÜSÜ

CMS İLERİ HADRON KALORİMETRESİ İÇİN DÖRT ANOTLU FOTOÇOĞALTICI SİMÜLASYONU

YÜKSEK LİSANS TEZİ

Mete YÜCEL
(509101131)

Fizik Mühendisliği Anabilim Dalı

Fizik Mühendisliği Programı

Tez Danışmanı: Doç. Dr. Kerem CANKOÇAK

MAYIS 2012

Mete YÜCEL, a M.Sc. student of ITU Graduate School of Science 509101131 successfully defended the thesis entitled **"SIMULATION OF FOUR ANODE PHOTOMULTIPLIERS FOR THE CMS FORWARD HADRON CALORIMETER"**, which he prepared after fulfilling the requirements specified in the associated legislations, before the jury whose signatures are below.

Thesis Advisor :	**Assoc. Prof. Dr. Kerem CANKOÇAK** Istanbul Technical University	.....
Co-advisor :	**Dr. Taylan YETKİN** The University of Iowa	.....
Jury Members :	**Prof. Dr. Cenap Ş. ÖZBEN** Istanbul Technical University	.....
	Assoc. Prof. Dr. İskender REYHANCAN Istanbul Technical University	.....
	Assist. Prof. Dr. Ferhat ÖZOK Mimar Sinan Fine Arts University	.....

Date of Submission : **4 May 2012**
Date of Defense : **8 June 2012**

FOREWORD

I would like to thank to my advisor Doç. Dr. Kerem Cankoçak for giving me the opportunity to go to CERN and work in this project and to my co-advisor Dr. Taylan Yetkin for his endless support and guidance.

I would also like to thank to my colleges Esra Barlas and Hüseyin Bahtiyar for their constant support and help.

In addition I would like thank to rector of Istanbul Technical University Prof. Dr. Muhammed Şahin for accepting the CMS membership of ITU and to TAEK for their financial support.

May 2012

Mete YÜCEL
(Physics Engineer)

TABLE OF CONTENTS

Page

FOREWORD ..... **vii**
TABLE OF CONTENTS ..... **ix**
ABBREVIATIONS ..... **xi**
LIST OF TABLES ..... **xiii**
LIST OF FIGURES ..... **xv**
LIST OF SYMBOLS ..... **xvii**
SUMMARY ..... **xix**
ÖZET ..... **xxi**
1. INTRODUCTION **1**
1.1 LHC 1
1.2 Physics Goals of CMS 2
1.3 PMT Upgrade 3
1.4 Aim of The Study 3
2. THE COMPACT MUON SOLENOID (CMS) **5**
2.1 General Purpose of CMS 5
2.2 Magnet 6
2.3 Tracking System 6
2.4 Electromagnetic Calorimeter 7
2.5 Hadronic Calorimeter 7
2.5.1 Hadronic Barrel 8
2.5.2 Hadronic Endcap 9
2.5.3 Hadronic Outer 10
2.5.4 Hadronic Forward 10
2.6 Muon System 12
2.7 CMS Computing and Software 12
3. HF SHOWER LIBRARY **15**
3.1 HF PMT Upgrade 15
3.1.1 Specification of old and new PMTs 15
3.1.2 Advantages of new PMT 17
3.1.3 Implemantation 18
3.1.3.1 Implemantation in data acquisition 18
3.1.3.2 Implemantation in CMSSW 18
3.2 Showers 19
3.2.1 Electromagnetic showers 19
3.2.2 Hadronic showers 20
3.2.3 Quartz fiber calorimeters 21

3.2.3.1 Working principle 21
3.2.3.2 Advantages of quartz fiber calorimeters 22
3.3 Simulation of HF PMT 23
3.3.1 HF GFlash 23
3.3.2 Shower Library 24
3.3.2.1 Constructing Shower Library 24
3.3.2.2 Old and new Shower Library 25
4. RESULTS AND CONCLUSIONS 27
4.1 Results of HF Shower Library 27
4.1.1 Old Shower Library 27
4.1.2 New Shower Library 29
4.2 Conclusion 29
REFERENCES 31
APPENDICES 33
APPENDIX A 34
APPENDIX B 45
CURRICULUM VITAE 47

ABBREVIATIONS

AOD	**:** Analysis Object Data
CERN	**:** European Nuclear Research Organization
CMS	**:** Compact Muon Solenoid
CMSSW	**:** CMS Event Reconstruction Software
CPU	**:** Central Processor Unit
HB	**:** Hadronic Barrel
HCAL	**:** Hadronic Calorimeter
HE	**:** Hadronic Endcap
HF	**:** Hadronic Forward
HO	**:** Hadronic Outer
LHC	**:** Large Hadron Collider
PMT	**:** Photomultiplier Tube
RECO	**:** Reconstruction
RMS	**:** Root Mean Squared

LIST OF TABLES

Page

Table 4.1 : Comparison of simulation with 5000 and 50000 events in Long fiber. 28
Table 4.2 : Comparison of simulation with 5000 and 50000 events in Short fiber. 28
Table A.1 : Mean and RMS of number of photon-electrons produced by electrons 41
Table A.2 : Mean and RMS of number of photon-electrons produced by pions ... 42
Table A.3 : Comparison of mean and RMS of number of photo-electrons produced by electrons between old and new PMT 43
Table A.4 : Comparison of mean and RMS of number of photo-electrons produced by pions between old and new PMT 44

LIST OF FIGURES

Page

Figure 1.1 : LHC and its detectors [1]. 2
Figure 2.1 : Detailed wiev of CMS structure [2]. 6
Figure 2.2 : Longitudinal view of CMS, showing HCAL subdetectors [3]. 7
Figure 2.3 : Transverse view of HB, showing wedge numbering [3]. 8
Figure 2.4 : η distribution of HB, HE and HO [3]. 9
Figure 2.5 : HF wedge [4]. 10
Figure 2.6 : Detailed view of HF design [3]. 11
Figure 2.7 : CMS tier centers workflow [3]. 13
Figure 3.1 : Hamamatsu R7525 PMT covered with black tape [5]. 16
Figure 3.2 : Hamamatsu R7600U-200-M4 [6]. 16
Figure 3.3 : Quantum efficiency difference of old and new PMT. 17
Figure 3.4 : Ratio of quantum efficiencies. 18
Figure 3.5 : Gain difference of old and new PMT [6], [7]. 19
Figure 3.6 : Radiation lengths to capture electromagnetic showers in different materials [8]. 20
Figure 3.7 : Nuclear interaction lengths to capture hadronic showers in iron [8]. . 21
Figure 3.8 : Trapping angle of Cherenkov photons [9]. 22
Figure 3.9 : Histogram of the number of photoelectrons produced in PMT by 100 GeV electrons, stored in the simulation ROOT file. 24
Figure 3.10 Old Shower Library ROOT structure and the histogram of the number of photoelectrons produced in PMT for all energies. 25
Figure 4.1 : Quantum efficiency difference of old and new PMT. 28
Figure A.1: Comparison of photo-electrons produced in electron simulation for existing old Shower Library and newly produced old Shower Library : Long fiber (a). Short fiber (b). 34
Figure A.2: Comparison of photo-electrons produced in pion simulation for existing old Shower Library and newly produced old Shower Library : Long fiber (a). Short fiber (b). 35
Figure A.3: Comparison of photo-electrons produced in electron simulation for two sets of newly produced data with 50000 events : Long fiber (a). Short fiber (b). 36
Figure A.4: Ratio of produced photo-electrons means's for each energy bin: For electrons (a). For pions (b). 37
Figure A.5: Ratio of produced photo-electrons RMS's for each energy bin: For electrons (a). For pions (b). 38
Figure A.6: Comparison of photo-electrons produced in electron simulation for old and new Shower Library: Long fiber (a). Short fiber (b). 39

Figure A.7: Comparison of photo-electrons produced in pion simulation for old and new Shower Library: Long fiber (a). Short fiber (b)..... 40

LIST OF SYMBOLS

α : Alpha
η : Eta
γ : Gamma
λ : Lambda
μ : Mu
π : Pi
ϕ : Phi
θ : Theta

SIMULATION OF FOUR ANODE PHOTOMULTIPLIERS FOR THE CMS FORWARD HADRON CALORIMETER

SUMMARY

Large Hadron Collider located in CERN is the world's biggest particle collider. Main design purpose of the LHC is to accelerate protons and collide them at the scale of TeV center of mass energy so that it allows physicist to study new physics beyond Standard Model predictions at that scale. LHC houses four big experiments and detectors. From these detectors ATLAS and CMS are general purpose experiments, ALICE is for studying quark-gluon plasma and LHCb is for studying b meson physics.

The detectors in the experiment will go through a maintenance in 2013. Some parts of the CMS(Compact Muon Selenoid) detector will be upgraded in this period. One of the changes that going to happen will be the PMTs of Hadronic Forward Calorimeter. The improvement will be achieved with this upgrade will help the data analysis for the physics processes that looked in the experiment.

Currently used PMTs are Hamamatsu R7525 models. This PMT has a borosilicate window and a bialkali cathode. It is very susceptible to the window hit events, where a coming particle made Cherenkov radiation in the PMTs window, resulting in anomalous events. Proposed new Hamamatsu R7600U-200-M4 PMTs hoped to decrease this anomalous events and make the energy resolution better. The new PMT has a borosilicate window and an ultra bialkali cathode. It has a thinner window that decreases the number of window hit events.

It is essential to make necessary adjustments for the used methods, for the new PMTs. Since the new PMT has four anodes, the readout scheme for it will be different than the old PMT, that has one anode. The different readout and the characterization of new PMTs must be represented in the CMS reconstruction software and the new PMTs must be simulated.

The new PMTs quantum efficiency function is generated and placed in the CMS reconstruction software. Problems related to the new version of the software and the misconfiguration of PMT geometry is solved.

For the simulation of HF PMT's, there are several options available. From the available methods, the HF Shower Library method was chosen to simulate HF PMTs. Shower Library contains the information about the created showers for different particles hitting the HF detector. These information then used when similar situation occurs, instead of doing a full simulation. Shower Library is created according to the existing Shower Library's template for the sake of compatibility.

A comparison between the old Shower Library and new Shower Library has been made. The differences were represented and explained. For future studies, the possible contribution of new PMTs to the physics analysis was discussed.

CMS İLERİ HADRON KALORİMETRESİ İÇİN
DÖRT ANOTLU FOTOÇOĞALTICI SİMÜLASYONU

ÖZET

Avrupa Nükleer Araştırma Merkezi(CERN)'de bulunan Büyük Hadron Çarpıştırıcısı(LHC) dünyanın en büyük parçacık çarpıştırıcısıdır. Parçacık demetleri birbirlerine ters yönde dairesel olarak hızlandırılıp detektörlerin içinde çarpıştırılmaktadır. LHC'de dört büyük detektör ve deney yer almaktadır. Bunlardan ATLAS ve CMS tüm fizik konularını araştırırken, ALICE deneyi kuark-gluon plasmayı, LHCb ise b-kuark hakkında araştırma yapmaktadır.

Bu deneylerden CMS ve onun hadron kalorimetresi bu tez çalışmasının üzerine yapıldığı kısımlardır. CMS detektörü parçacıkların konumunu saptayan bir iz sürücü, elektromanyetik etkileşimleri ölçen bir elektromanyetik kalorimetre, hadronik etkileşimleri ölçen bir hadronik kalorimetre ve müonları saptamak için yapılan ve detektöre de ismini veren müon odalarından oluşmaktadır. Bütün parçalarıyla CMS hermetik bir detektör olup her bölgeden gelen parçacıkları saptayabilmektedir.

İz sürücü silikon piksel ve şerit detektörlerden oluşmakta olup, çarpışma noktasından sadece 4.4 cm uzaklıkta bulunmaktadır. İz sürücüler parçacıkların çarpışma verteksinden dağıldıkları yolları saptayarak, parçacıkların çarpışma sonrası yörüngelerinin belirlenmesinde kullanılmaktadır.

Elektromanyetik kalorimetre, iz sürücünün dışında bulunmaktadır ve elektromanyetik olarak etkileşen parçacıkların enerjilerini bıraktıkları bölgedir. Aynı şekilde elektromanyetik kalorimetrenin dışında, hadronik kalorimetre vardır ve bu kalorimetrede hadronik parçacıkların enerjilerini detektörde bıraktıkları yerdir. Bu iki kalorimetrenin de merkezde ve yanlarda, çarpışma noktasının her iki tarafında parçaları vardır. Ek olarak hadronik kalorimetrenin, ileri bölge olarak tanımlanan, çarpışma noktasından 11.2 m ötede de bir parçası vardır.

İz sürücü, elektromanyetik kalorimetre ve hadronik kalorimetre CMS'in mıknatısının içinde yer almaktadır. Bu mıknatıs dünyadaki en büyük mıknatıs olup 4.8 T büyüklüğünde manyetik alan yaratabilmektedir.

Müon odaları ise CMS mıknatısının dışından başlamaktadır. Bu parçacının tasarım amacı zor etkileşime giren müonları ölçmek olduğu için, kabul edilebilir ölçülerde, müonların etkileşimini maksimuma çıkarmak amacıyla olabildiğince büyük hazırlanmıştır.

CMS'in genel fizik amacı Higgs bozonunun var olup olmadığını araştırmaktadır. Bu parçacık maddenin nasıl kütle kazandığı sorusuna açıklama getirmek için gereklidir. Bu keşif ayrıca Standart Modelinde doğru olup olmadığı konusunda bilgi verecektir. Bu parçacık haricinde CMS'de süpersimetri, ekstra boyutlar ve daha pek çok standart model ötesi modellerin testleri ve bu modellere ait parçacıların bulunmalarına yönelik

çalışmalar yapılmaktadır. Ayrıca alınan verilerle Standart Modelin daha kesin sonuçlarla tekrar doğrulanması da önemlidir.

Bütün bu analizler ve veri alımı işlemlerinin aksamadan yapılabilmesi için CERN'in ve CMS'in yeterli bir bilgisayar ağı altyapısına sahip olması gerekmektedir. Bu konuda CERN, hem kendi içinde hem de dışarıdan eriştiği büyük bir bilgisayar ağına sahiptir. Kullanıcılar bu ağdaki bilgisayarlara bağlanarak analizlerini ve işlerini yapabilmektedirler. CMS içindeki işlerin yapılabilmesi içinde CMSSSW adında bir yazılım paketi kullanılmaktadır. C++, Python ve Geant4 temelli olan bu yazılım, tezdeki analizlerin yapılması için kullanılmıştır.

Türkiye'de dahil olmak üzere Dünya üzerinden pek çok ülkenin de katkıda bulunduğu LHC deneyi ve dahilindeki detektörler 2013 yılında bakım çalışmaları altına girecektir. Deneyin durakladığı bu evrede CMS detektörünün bazı kısımlarında çeşitli yenileme çalışmaları da olacaktır. Bu yenileme çalışmalarından biride İleri Hadron Kalorimetresindeki(HF) foto çoğaltıcı tüplerin(Photomultiplier tube) değiştirilmesidir. Eski foto çoğaltıcıların sahip olduğu sorunlar ve verim kaygıları, yeni bir foto çoğaltıcı arayışını doğurmuştur. Yeni foto çoğaltıcıların takılması ile CMS deneyinin fizik analizlerinde iyileşme sağlaması beklenmektedir.

İleri Hadron Kalorimetresi çarpışma noktasından 11.2 m ötesinde bulunan ve ileri bölgeye gelen jetlerin ve parçacıkların enerjilerini kaybettikleri kalorimetredir. CMS detektörünün simetrik şekilde iki tarafında birer disk şekilinde bulunan HF + ve HF - detektörlerinin her biri pasta dilimi şekilinde, 20 dereceye eşdeğer 18 parçadan oluşurlar. HF bir kuartz fiber kalorimetresidir ve gelen parçacıkların detektörde oluşturdukları duşlardan gelen parçacıkların, detektör içindeki fiberlerde Cherenkov radyasyonu oluşturmasıyla çalışır. Fiberlerde üretilen fotonlardan bir fotoçoğaltıcı tüp vasıtasıyla foto-elektronlar üretilir. Üretilen foto-elektronlar ışık toplayıcılarıyla elektronik okuma ünitelerine transfer edilirler ve burdan bir sinyal okunur. Her bir elektronik okuma ünitesi kutusunda 24 tane fotoçoğaltıcı bulunur. Fotoçoğaltıcıların 2 HF'te iki uzun ve kısa olmak üzere iki tip fiber vardır. Farklı iki fiberden gelen sinyallerin karşılaştırılması ile parçacıkların hadronik veya elektromanyetik etkileşen parçacıklar oldukları saptanabilir. Elektromanyetik parçacıklar kolay etkileşime girdiklerinden detektörün tüm boyunu giden uzun fiberlerde sinyal verirler. Öte yandan hadronik parçacıklar daha geç etkileşmeye başlarlar, böylelikle hem uzun fiberlerde hem de detektörün ön tarafından 22 cm sonra başlayan kısa fiberlerde sinyal verirler.

Şu an HF detektöründe kullanılan foto çoğaltıcılar Hamamatsu'nun R7525 modelidir. Bu modelde borosilikat cam ve bialkali katot tipi kullanılmıştır. Bu cihazlar cama çarpma olaylarına maruz kalmaktadırlar. Cama çarpma olayları gelen parçacıkların foto çoğaltıcının camında Cherenkov radyasyonu yaymaları ve detektörde sahte bir sinyal oluşturması demektir. Önerilen yeni Hamamatsu R7600U-200-M4 foto çoğaltıcılarda borosilikat cam ve ultrabialkali katot bulunmaktadır. Bu foto çoğaltıcılarının cam bölgesi daha ince olduğundan dolayı, bir parçacık cama çarpıp Cherenkov radyasyonu yarattığında daha az sinyal verecektir ve dolayısıyla bu sahte sinyaller azalacaktır. Ayrıca yeni foto çoğaltıcılar daha korunaklı dış yapıları sayesinde başka parçacıklarla olan etkileşimlerini de azaltacaklardır.

Bahsedilen tarzda istenmeyen sinyallerin kesilmesi haricinde yeni foto çoğaltıcıların yüksek kuantum verimleri ve çok anotlu olmaları sebebiyle enerji çözünürlüğünde de bir iyileşme sağlanacaktır. Dört anotlu bu foto çoğaltıcılar, eskilerin aksine dört

farklı kanaldan sinyal verebilmektedir. Bir olayda sinyalin hangi çıkışlardan geldiği takip edilmesi ve bu konuda seçimler yapan algoritmalar yazılması, olay seçiminde de iyileşmelere neden olacaktır.

Çalışır halde bulunan sistemin yeni çok anotlu foto çoğaltıcılarla göre ayarlanması önem arz etmektedir. Tek anotlu olan eski foto çoğaltıcılara nazaran yeni foto çoğaltıcıldan alınan sinyalin de okunması eski foto çoğaltıcılara göre farklılık gösterecektir. Bu farklı okuma tarzı ve yeni foto çoğaltıcının özellikleri CMS yeniden yapılandırma yazılımında(CMSSW) tanımlanmalıdır. Sonrasında ise yeni foto çoğaltıcı ile ilgili simülasyonlar yapılmalıdır.

Yeni foto çoğaltıcıların kuantum verimlerini(Quantum efficiency) tarif eden fonksiyon parametrize edilmiş, foto çoğaltıcının çalışma dalga boyundaki aralıklara göre bölünmüş ve CMSSW sisteminde HF detektöründeki Cherenkov radyasyonu hesaplamalarıyla ilgili parçacının içine yerleştirilmiştir. Bu aşamada ortaya çıkan, yeni bir yazılım sürümü kullanmakla alakalı hatalar ve foto çoğaltıcı geometrisinin Geant4'de yanlış tanımlanmış olmasından kaynaklanan sorunlar giderilmiştir.

HF ve foto çoğaltıcı simülasyonu için farklı seçenekler vardır. Bunlar sırasıyla tam Geant4 simülasyonu yapmak, HF GFlash yöntemini kullanmak yada Shower Library metodunu kullanmaktır. Tam Geant4 simülasyonu yapmak çok zahmetli ve HF GFlash yöntemi de gene başka yollarla elde edilecek parametrizasyon verilerine bağımlı olduğu sebebiyle, yeni foto çoğaltıcıların simülasyonlarının yapılabilmesi için Shower Library metodu seçilmiştir.

Shower Library kalorimetrede oluşan hadronik ve elektromanyetik duşların daha kolay simüle edilebilmesi için hazırlanmış bir yöntemdir. Farklı enerjilerdeki farklı parçacıkların oluşturdukları duşların verileri üretilerek Shower Library adı altında bir elektronik kütüphane dosyasında saklanır. Böylelikle daha sonra bir duş simüle edilmesi gerektiği zaman, sistem Shower Library'e erişerek daha kısa ve daha verimli bir şekilde, neler olacağını söyleyebilir. Bu işlem hız ve güç kazanımı yanında, bir seçenekten başka bir seçeneğe geçme işlemini de kolaylaştırmaktadır. Foto çoğaltıcıların değişmesi durumunda farklı foto çoğaltıcılar için yazılmış kütüphaneler kullanılarak ana programları değiştirmeden sonuç alınabilinir.

Bu çalışma için eski Shower Library formatına uyularak yeni Shower Library baştan yaratılmıştır. Eski şablonun takip edilmesi program içinde uyumluluk sağlaması düşücesiyle kararlaştırılmıştır. Bu esnada eskiden yaratılmış olan Shower Library'nin çok eski bir CMSSW sürümü ile yaratılmış olmasından kaynaklı sorunlarda giderilmiştir. Yeni CMSSW sürümleri için uyumlu olarak yazılan program, başka kullanıcılarında bu metodu kullanmak isteyebilecekleri göz önüne alınarak hazırlanmıştır.

Eski ve yeni Shower Library arasındaki farkların gösterilmesi amacıyla sonuçlar hazırlanmıştır. İlk etapta yapılan değişikliklerin, eski sonuçları tekrar edip edemediği test edilmek istenmiştir. Shower Library metodu geliştirildiğinde eski foto çoğaltıcılar için hazırlanan Shower Library sonuçları alınmış ve gene eski foto çoğaltıcılar için yeni CMSSW sürümü ve yeni Shower Library kodu kullanılarak elde edilen sonuçlarla karşılaştırılmıştır. Elde edilen sonuçlarda uyum görülmüş, daha düşük bir hata ile simülasyonun yapılabilmesi için daha fazla simülasyon verisine ihtiyaç duyulduğu gösterilmiştir. Daha sonra yeni foto çoğaltıcılar için sonuçlar çıkarılmış, yüksek kuantum veriminden dolayı oluşan daha fazla foto-elektron sayısı gözlenmiştir.

Gelecek çalışmalar için yeni foto çoğaltıcıların fizik analizlerine getirebileceği etkiler tartışılmıştır. Foto çoğaltıcıların ve foto çoğaltıcıların okunma şekillerinin değişmesi fizik analizlerinde iyileşme yada kötüleşmeye sebep olacaktır. Bu etki çok küçük bir değişime sebebiyet vereceğinden, hassas ölçümün önemli olduğu ve Standart Model ardalanlarının etkisinin büyük olduğu çeşitli Standart Model ötesi fizik çalışmalarında önemli olacaktır.

1. INTRODUCTION

European Organization for Nuclear Research (CERN) is the central place for today's experimental and theoretical physicists to study particle physics. It houses the world's biggest and capable particle accelerator to date, the Large Hadron Collider (LHC) still could not reach its potential and will go into maintenance in 2013, when all of the experiments will put to a hold. During this time period, photomultiplier tubes of forward hadronic calorimeter at CMS will be changed. Simulation and testing of these new photomultipliers are important for the calorimeter to work properly. CMS event reconstruction software (CMSSW) needs to be updated for the parts concerning photomultipliers.

1.1 LHC

LHC (Large Hadron Collider) is the world biggest circular synchrotron located at the Swiss-France border near Geneva. LHC was built 100 m beneath the surface of earth and its circumference is about 27 km. Main design purpose of the LHC is to accelerate protons and collide them at the scale of TeV center of mass energy so that it allows physicist to study new physics beyond Standard Model predictions at that scale. LHC also collides heavy ion beams to study QCD (Quantum Chromodynamics) matter at high energies [10].

LHC has various detectors at specific points on its tunnel shown in Figure 1.1. From these detectors ATLAS and CMS are general purpose experiments which includes the search for Higgs boson and beyond standart model theories. From the other two detectors, ALICE is for studying quark-gluon plasma and LHCb is for studying b meson physics. All the work done in this thesis are performed within CMS collaboration, specifically in the hadronic calorimeter of the CMS, therefore the CMS detector and its subdetectors will be explained in detail.

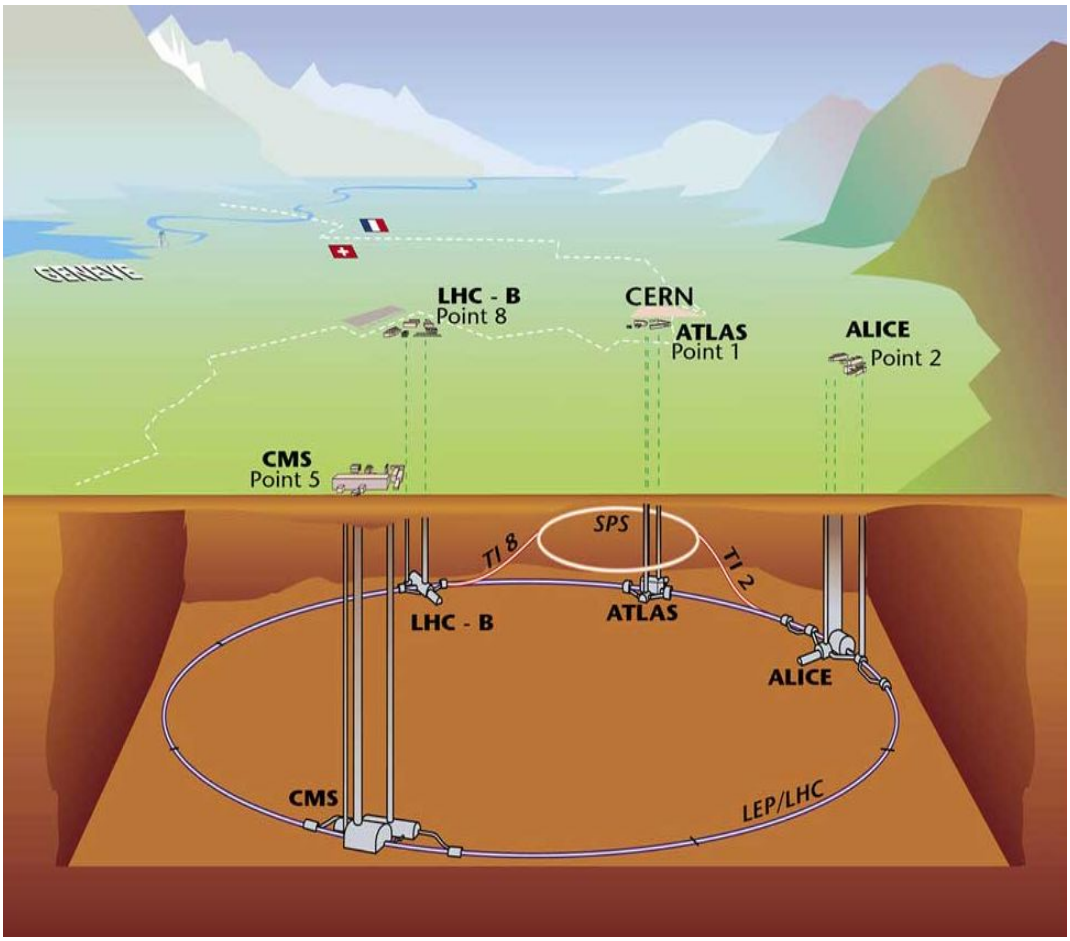

Figure 1.1: LHC and its detectors [1].

1.2 Physics Goals of CMS

Even if the CMS is a general purpose experiment, its main goal in the near future is to find the Higgs particle. The detector was designed to this end to search most probable physics channels. Examples for these channels are :

$$H \rightarrow ZZ \rightarrow 4\mu \tag{1.1}$$

$$H \rightarrow \gamma\gamma \tag{1.2}$$

Muon system and electromagnetic calorimeter were built some of these channels in mind.

However, these discovery channels cross sections are quite small compared to other Standard Model physics channels. Even if there is enough data to find Higgs particle, without the proper detection of Standard Model,which are background events, the discovery channels can not be claimed. That is why it is also a equally important goal for CMS to observe Standard Model predictions with precision.

For example, it is very important for CMS to correctly measure QCD jets and missing energy. In the channel of

$$H \rightarrow bb \tag{1.3}$$

the background almost dominated with QCD $b\bar{b}$ production [11].

1.3 PMT Upgrade

LHC has been operated at 7 TeV center of mass energy in 2011. It will reach to the 8 TeV center of energy in 2012. These energies, however, are still far behind what is previously planned as a goal of 14 TeV center of mass energy. To achieve this goal both the performance of LHC should be maintained and there needs to be made improvements.

The decision process for upgrade on the detector part themselves is a very critical topic. Most of the detector components cannot be changed without stopping the experiment, the decision must be made beforehand to not to delay the experiments schedule. There is an extensive amount of time needed to wait for radiation levels in the detector caves become safe. Even after that detectors cannot be disassembled easily. Once the update is completed and experiment starts, it will be very hard to correct the mistakes done during the upgrade process.

To prevent such things and make the right upgrade choices, all of the upgrade plans are frequently discussed and tested. There are more than one test site at CERN to research upgrade work. A lot of components are tested on these sites before making a decision and investments. Also some of the new components that may be used in future are tried in the actual detectors. The new photomultiplier tubes that will be used for HF calorimeter are also tested in these sites.

1.4 Aim of The Study

Aim of CMS experiment is to look into the physics processes and to test and study physics models. Considering this scheme, all the work done here is to help to achieve these goals. An upgrade study will be made for the HF detector and its effect on the known physics processes will be shown. The improvements made on the analysis make the search for other important physics processes easier. The known physics processes

that produce a background for the searched physics will be excluded better. It will also give a performance test for the new PMTs.

Overall in the course of this study, how the HF PMT upgrade became possible and how it effects the physics analysis will be examined.

2. THE COMPACT MUON SOLENOID (CMS)

In this chapter, the CMS detector's structure, its working principle and computing framework will be explained.

2.1 General Purpose of CMS

CMS (Compact Muon Solenoid) experiment is located on the LHC tunnel, beneath 100 meter of Cessy Village. It is roughly 22 meters in length and 15 meters in diameter with a mass of 12.500 t. CMS from the ground up is designed to be a compact and high granularity detector with fast response time. With 25 ns bunch crossing time, it is hard to differentiate the events from each other, and without a detector with a response time better than 25 ns, pile up is unavoidable. Because of this, CMS has very high number of detector channels with good time resolution. CMS's coordinate system is taken as beam direction coming from the LHC Point Five toward the Jura Mountains as positive z axis. Coordinate system origin is at the interaction point at center of CMS. From this point, vertical upwards is positive y axis and radially inward is x axis. Azimuthal angle ϕ is measured from x axis in the x-y plane and the polar angle θ is measured z axis in the z-y plane. However to specify detector geometry, psuedorapidity is being used rather than θ. Psuedorapidity is defined as $\eta = -\ln\tan(\theta/2)$ [3].

CMS consists of several layers as seen in Figure 2.1. Around the interaction point, where particles collide, is tracker system. Outside the tracker, there is an electromagnetic calorimeter. After the location where electromagnetic calorimeter ends, hadronic calorimeter starts and stretches as far as to superconducting magnet that surround it all. Immediately above from the solenoid is the outer hadronic calorimeter. Outside, there is an iron yoke and muon chambers between its layers. There is also forward calorimeters at the two ends of CMS, covering a very high psuedorapidity range close to the beam pipe.

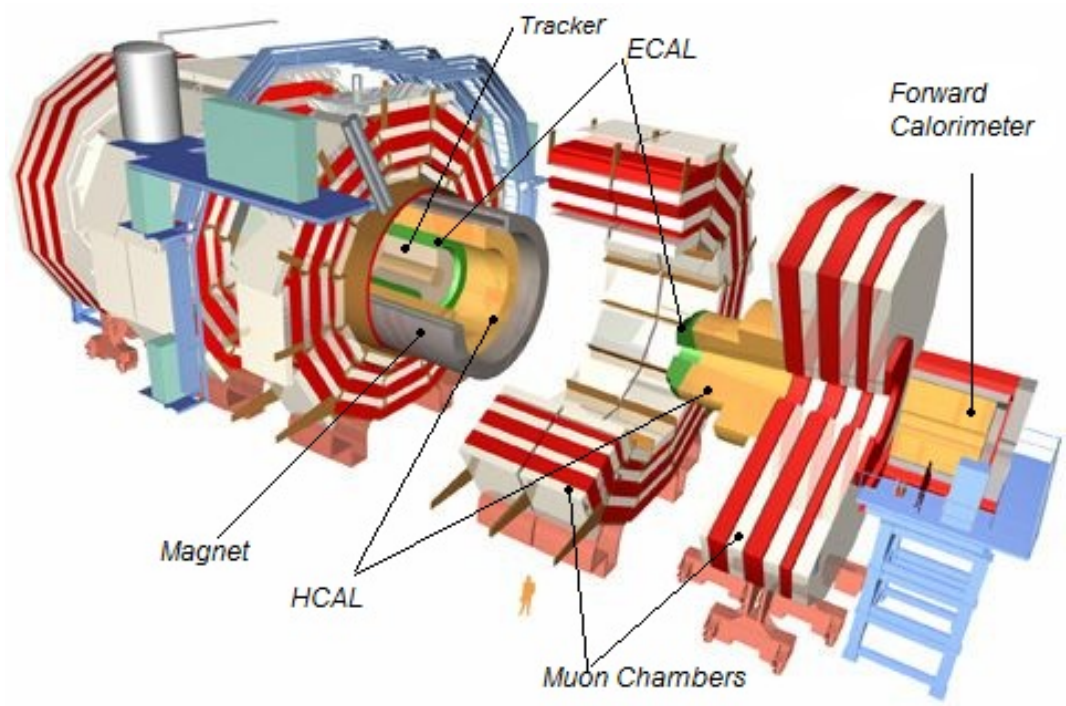

Figure 2.1: Detailed wiev of CMS structure [2].

2.2 Magnet

Magnet used in CMS is a superconducting solenoid that can produce a large bending power at 4 T magnetic field. Magnet bends the muons before they enter the muon system, and from the curvature angle of muons their momentum and energy are calculated.

Superconducting magnet is a very large structure. It is 12.5 m in length and has a 6.3 m inner diameter. It can store 2.6 GJ energy when the current is maximum and it inducts 14 H magnetic field. Solenoid is made of NbTi conductors and consist of four layers of winding. It is placed inside the cryostat that keep the temperature at 1.8 K. It has a mass of 220 t and with the iron yoke that surrounds it, total mass of the magnet system is higher than 10.000 t [3]. As of 2012 , the CMS magnet operates at 3.8 T.

2.3 Tracking System

Tracking system of CMS is built to measure the trajectories of charged particles. Tracker has 5.8 m length and 2.5 m diameter and it is located 4.4 cm around the interaction point. Since the interaction rate of LHC is very high and the tracker is so close to the interaction point, the intense particle flux can do high radiation damage to the tracker in the long term of operating of LHC. To make sure that signal to noise

ratio of tracker remains above 10 for at least 10 years, pixel detectors and silicon strip trackers are being used. There are 1440 pixel and 15.148 strip detector modules in the tracker system [3].

2.4 Electromagnetic Calorimeter

Electromagnetic Calorimeter consists of 68.524 lead-tungstate (PbWO4) crystals. These crystals are located in the barrel region of ECAL that covers the psuedorapidity range < 1.479 and endcap region of ECAL in the psuedorapidity range of 1.479 < 3.0. Since these crystals have high density (8.28 g/cm^3) and short radiation length (0.89 cm), ECAL is a compact calorimeter and have high granularity [3].

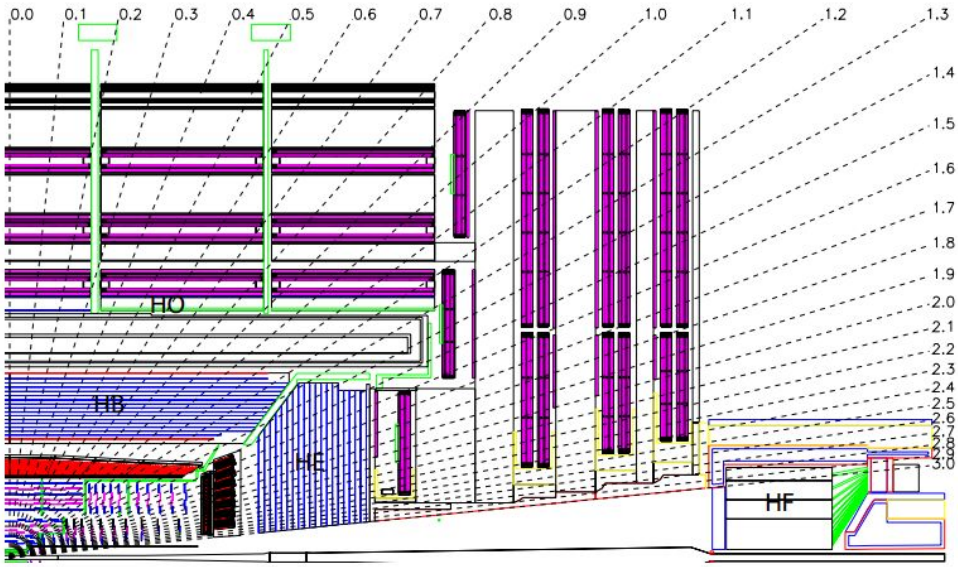

Figure 2.2: Longitudinal view of CMS, showing HCAL subdetectors [3].

Lead tungsten crystals are also very fast. The scintillation decay time of crystals is in the order of magnitude of LHC bunch crossing time, which is 25 ns. Usually scintillation wavelength of crystal is between 420-430 nm and for the detection of the scintillation light avalanche photodiodes and vacuum phototriods are being used [3].

2.5 Hadronic Calorimeter

Hadronic calorimeter is the part of the detector that can detect hadrons. It is very important to observe and analyze jets, missing transverse energy and a lot of type of particles coming from the diverse final states of collision. Jets are particularly

important objects that must be correctly constructed so with missing transverse energy signals they can be used to find many new physics searches.

HCAL is located between the ECAL and the CMS magnet. It has a barrel region calorimeter (HB), endcap region calorimeter (HE), and forward region calorimeter (HF). There is also an outer calorimeter, called HO, for the purpose of catching showers happens late after HCAL barrel region, outside of CMS magnet. Therefore HB, HE and HO covers to the psuedorapidity region $|\eta| = 3$ and beyond that forward calorimeter HF covers until $|\eta| = 5.2$, as seen in Figure 2.2.

One of the biggest contributions to CERN experiment from Turkey is for HCAL. This thesis also focus on the work done on HCAL, therefore all of the HCAL's sub detectors will explained in detail.

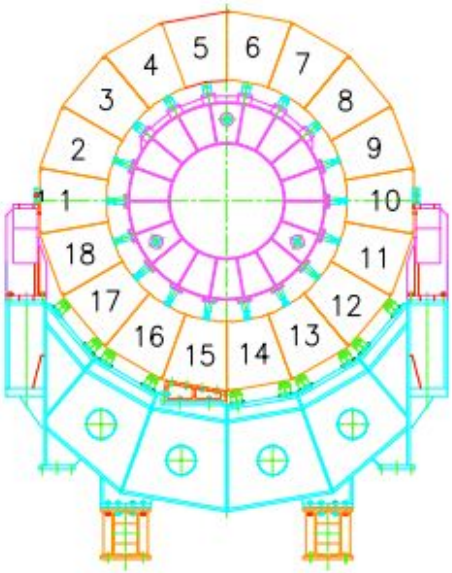

Figure 2.3: Transverse view of HB, showing wedge numbering [3].

2.5.1 Hadronic Barrel

Barrel region of HCAL is constructed with 36 wedges, placed in azimuthal direction (Figure 2.3). 18 wedge at the side of z+ direction called HB+ and the other 18 wedge at the side of z- called HB-. Absorber has 40 mm thick steel plate in the front layer and a 75 mm thick in the latest layer and in-between, there are brass plates varying between 50.5 mm and 56.5 mm thickness. On the other hand HB+ and HB- both divided into 16 sectors in η. These sectors called towers. Final resolution in polar and azimuthal angle is $\Delta\eta = 0.087$ and $\Delta\phi = 0.087$ [3].

The scintillator material of the CMS is 3.7 mm thick Kuraray SCSN81. When signal comes out from scintillator it is carried to a hybird photodiode (HPD) by wavelength shifting fibers. HPD have a photocathode working at -8kV high voltage. With a photoelectron passing through the diode, gain of the HPD becomes approximately 2000. There is also one more cable coming to the HPD. This cable carries laser or LED light and data taken from these signals used to calibrate and maintain the HPD gain [3].

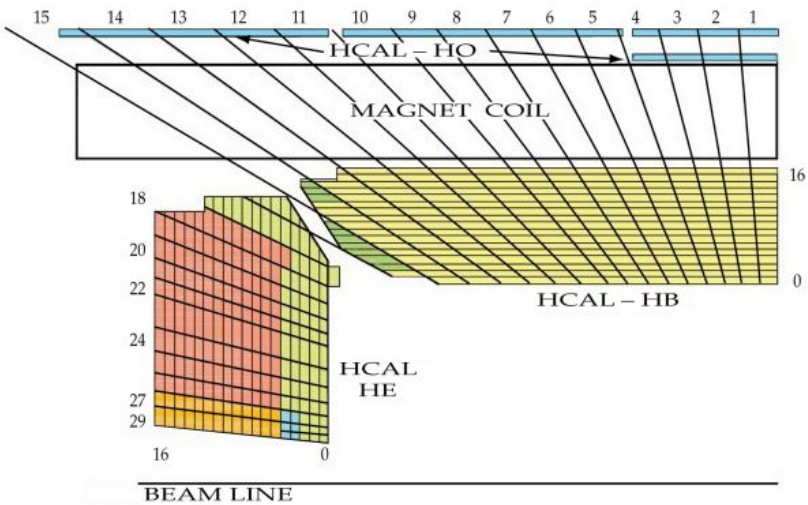

Figure 2.4: η distribution of HB, HE and HO [3].

2.5.2 Hadronic Endcap

Endcap calorimeters are placed like plugs in either side of HB and attached to the muon systems yoke. They cover the region $1.3 < |\eta| < 3$ and tower numbered 16 overlaps in HE and HB. HE towers goes from 16 to 29. η distribution of towers in HB and HE is in Figure 2.4. Granularity of HE is $\Delta\eta = 0.087$, $\Delta\phi = 0.087$ for $|\eta| < 1.6$ and $\Delta\eta = 0.17$, $\Delta\phi = 0.17$ for $|\eta| \geq 1.6$ [3].

HE is designed so it can minimize the space between HB and HE so no particle can escape through. Its build material C26000 cartridge brass is choosed for the interaction length, mechanical properties and low cost. Brass plates are 79 mm thick and following them are scintillators. Multipixel hybrid photodiodes are used for receiving scintillation. These photodiodes have low sensivity to magnetic fields so CMS magnet interfere less with the endcap region [3].

2.5.3 Hadronic Outer

In the barrel region EB (barrel region of electromagnetic calorimeter) and HB do not have the length to capture all of the hadronic shower. Because of this, HO is placed outside of CMS magnet and uses solenoid coil as an absorber and detect showers after HB. After solenoid there are scintillators tiles that made up the HO. Scintillators are made of Bicron BC408 at the thickness of 10 mm [3].

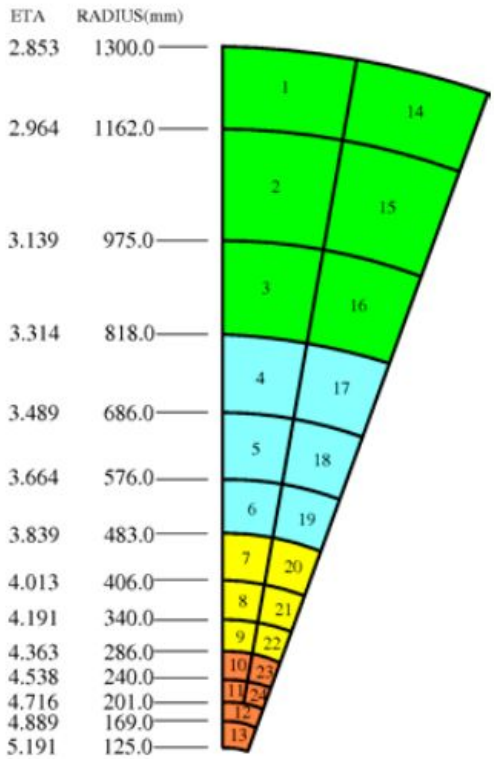

Figure 2.5: HF wedge [4].

The space HO has is constrained by muon system. It is placed at the first layer of muon systems yoke. HO has a similar η distribution to HB and it is divided into 5 rings along the η direction. Rings are numbered with -2, -1, 0, 1, 0 and they each divided into 12 ϕ sector. Overall granularity of towers is again like HB at $\Delta\eta = 0.087$ and $\Delta\phi = 0.087$ [3].

2.5.4 Hadronic Forward

The forward calorimeter is located 11.2 m away from the interaction point of CMS. It is a cylindrical calorimeter with a outer radius of 130 cm. HF is 12.5 cm away from the center of the beam line [3]. It is divided into 36 wedges with 18 of them being either

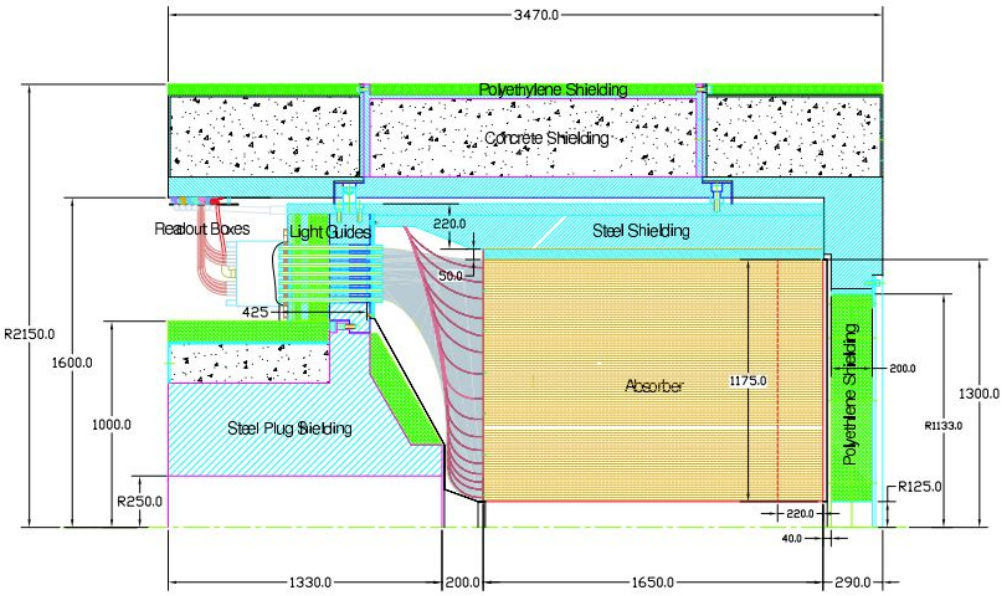

Figure 2.6: Detailed view of HF design [3].

side of the detector. Towers of HF has a granularity of $\Delta\eta = 0.175$ and $\Delta\phi = 0.175$. Transverse view o a HF wedge can be seen in Figure 2.5.

Even with the distance to the interaction point, HF is the most energy deposited part of the calorimeter. While average of 100 GeV energy deposited in the rest of the detector, HF has a average energy deposition of 760 GeV [3]. Also this energy distribution is not uniform and has its maximum at higher η. To work in this conditions for a long time, HF had to be built with a material that has good radiation hardness. Because of this quartz fibers are used as active material in HF.

HF has a steel absorber that is made of 5 mm thick grooved plates [3]. Quartz fibers are located in these grooves. There are two kinds of fibers in HF. So called long fibers starts from the front and goes full length of the absorber, that is 165 cm. On the other hand short fibers begin at 22 cm away from the front face of the absorber, so they are 143 cm long. With two different cable in length, hadronic and electromagnetic showers are differentiable. Electromagnetic showers usually give most of their energy in the first 22 cm of detector so they are mostly detected by long fibers. On the other hand hadronic showers starts a bit later than electromagnetic showers due to their more complex interaction and they are observed both in long and short fibers. The Cherenkov light produced in the quartz fibers are then carried by light guides to the photomultiplier tubes (PMT). The photomultiplier tube used is Hamamatsu R7525

that has a borosilicate glass window, single anode PMT. 24 of these photomultiplier tubes are stored in the read out box, covering half of a wedge. Detailed look of CMS is given in Figure 2.6.

All of the HF protected from the intense radiation with a hermetic shielding. Shielding materials are 40 cm thick steel, 40 cm thick concrete and 5 cm thick polyethylene. There is also a radiation damage monitoring system installed in HF to observe long time effects of integrated luminosity to the detector. The information comes from a few reference quartz fibers placed in the absorber [3].

2.6 Muon System

Muon system is the central part of the detector that give its name to the detector. CMS is designed from the beginning to have good muon measurement. This kind of ability is needed because one of the most probable channel to observe Higgs boson are

$$H \rightarrow ZZ \tag{2.1}$$

or

$$H \rightarrow ZZ^{*} \tag{2.2}$$

all have four muons coming out in their final states.

Muon system consist of drift tubes between the psuedorapidity region $|\eta|$<1.2. They are located in four different muon stations separated by flux return plates. At the endcap region of muon system covering the psuedorapidity range 0.9 <$|\eta|$ < 2.4, there are cathode strip chambers installed. There is also resistive plate chambers, located in both barrel and endcap region for better muon triggering [3].

2.7 CMS Computing and Software

One of the biggest challenges for a big experiment like CMS is that to have good computing framework. Obtaining all the information from the collisions, keeping them to analyze and allowing a lot of users to access this data in a daily basis for such a long time needs much effort.

CMS data model is based around the Event. Event allows to access information of a single bunch crossing. Moreover other data and objects can be derived from it such

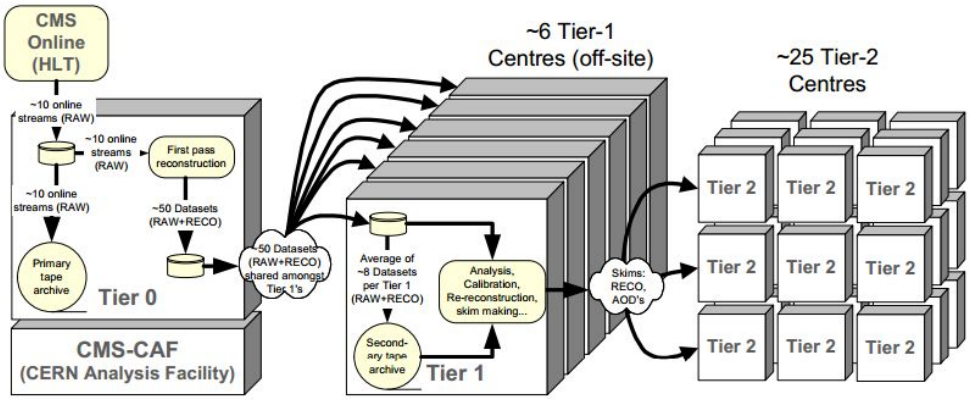

Figure 2.7: CMS tier centers workflow [3].

as digitized data, reconstructed data or other high physics data objects. Software of CMS, called CMSSW, enable users to produce, analyze, filter from Event objects. While doing so users can change the desired parameters editing the corresponding configuration files. For easy handling, events usually collected in event collections and they are stored in ROOT files. CMSSW is based on C++, Python languages and Geant4 detector simulation and it gives a strong framework [3].

Data taken in the CMS have several types. RAW data have all the recorded information from the collision and trigger information. System later tag these data to decide whether it is usable for analysis or not. Reconstructed data, so called RECO data are the data which gone through many algorithms to have high level physics objects. RECO data are suitable better for analysis due to its content and relative small size compared to RAW data. However it is also the most CPU (central processor unit) consuming process. AOD (analysis object data) are produced by filtering RECO data. It has even a lesser size than RECO and have sufficient amount of information to analyze [3].

CMS take data to its storages at the rate of 300 Hz for proton proton collisions. For one event this roughly takes 1.5mb. Because of this rapid data taking, a large storage medium is needed. This system should be also flexible so it can support a wide range of data processing methods. All of this cannot be done in the same place. CMS have several computing centers, categorized from Tier 0 to Tier 2 [3]. Workflow of these centers can be seen in Figure 2.7.

Tier 0 center is located at CERN. It stores RAW data to its permanent mass storage and produce the first-pass RECO datasets. Then it copies these data to Tier 1 centers. Tier 1 centers are located all around the world. Tier 1 stores a second copy of data from Tier 0. Its main purpose is to allow second-pass reconstruction and allow Tier 2 centers to take data to analyze. Tier 2 centers are located between the CMS institutes. It provides the space for users to carry out desired analysis and tasks [3].

3. HF SHOWER LIBRARY

The simulation of PMT's in HF is currently performed with two methods: HF GFlash and HF Shower Library. Users can choose whichever method they want in their simulation. However with planned PMT change for HF detector, HF Shower Library method should be modified accordingly to work with new PMTs. To update Shower Library, specifications and behavior of new PMT's, and the simulation background are needed and they will be explained in detail.

3.1 HF PMT Upgrade

HF has currently using the PMT model R7525 from Hamamatsu [5]. These PMT's are very susceptible to the anomalous events. These events includes PMT hits that are caused by particles coming from other places then fibers. The window hits in particular usually happen due to muons or punch through events [12]. Therefore HF needed some new PMT that will improve the event selection and energy resolution. Selected new PMT also needed to pass HF PMT requirements and should not change the basic PMT operation drastically [5]. To achieve this goals, R7600-U-200-M4 model from Hamamatsu has been proposed.

3.1.1 Specification of old and new PMTs

Current PMT (R7525), as seen in Figure 3.1, has a cylindrical shape with 28 mm in diameter and most of its surface surrounded with glass. The window glass used in this model is borosilicate, and its cathode type is bialkali. Proposed new PMT however (Figure 3.2) has a box like shape and has only one window at front. Active area of window active area is 18 mm to 18 mm and it uses borosilicate, and it uses ultra bialkali for the cathode. The window of new PMT is also thinner. Both PMT are sensitive between the 300-650 nm but the current PMT has a peak value of 420 nm and new PMT has a lower peak value of 350 nm.

Figure 3.1: Hamamtasu R7525 PMT covered with black tape [5].

New PMT has higher quantum efficiency than currently used PMT has (Figure 3.3). While old PMT's quantum efficiency has its maximum around it 20% with a photon wavelength sensivity of 400 nm, new PMT's has this around 40% with a photon wavelength sensivity of 330 nm, on average new PMTs have 1.7-1.8 times more quantum efficiency than old ones (Figure 3.4). New PMTs have also higher gain then current PMTs (Figure 3.5).

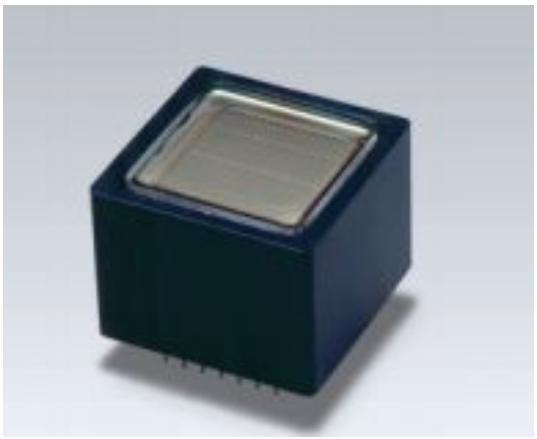

Figure 3.2: Hamamatsu R7600U-200-M4 [6].

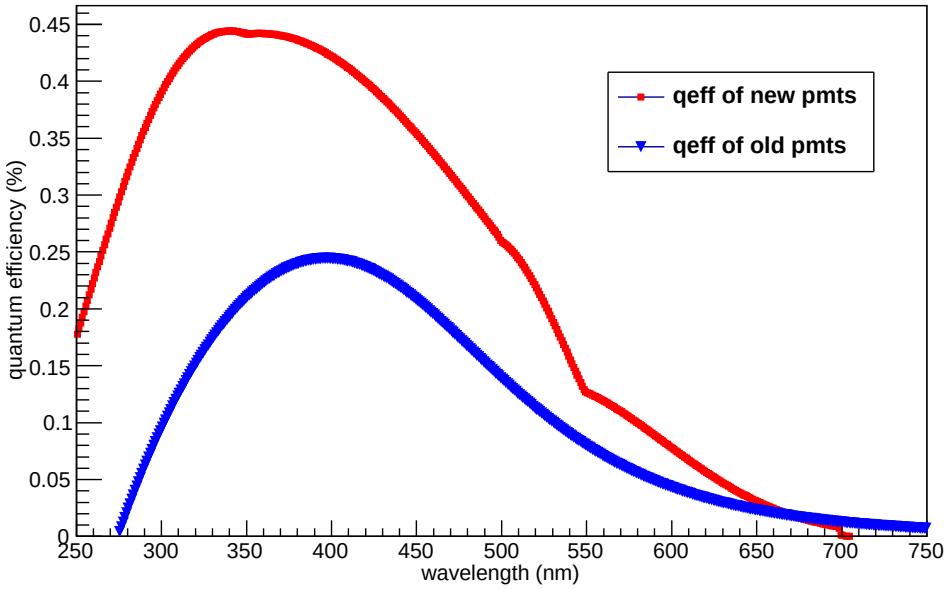

Figure 3.3: Quantum efficiency difference of old and new PMT.

Final important distinction between these two PMTs are their anode types. The older model R7525 is a single anode PMT whereas R7600-U is a multi anode PMT with four anodes. Since it has four anodes, reading the signal will be different in readout modules in HF.

3.1.2 Advantages of new PMT

There are several important advantages of new PMT over the old one. First is that it is a multi anode PMT. There are anomalous events in HF, some of which can be better eliminated with the new PMT. Some particles interact in the PMT window and produce fake signals. These signals can be identified better in new PMT by writing algorithms that compare the signals coming from different anodes. It also allows to correct the window hit energy. On the other hand since new PMT's window is thinner, it is less likely that particles interact within the window, and metal envelope of new PMTs reduces the window hitting events in comparison to body of old PMT [5].

Second important advantage is that it has more quantum efficiency and gain than the older PMT has. More quantum efficiency means there are more photo-electrons produced when photons hit the cathode, and more gain means that a clearer signal will come out from the PMT. Because of these effect the resolution of HF will be improved.

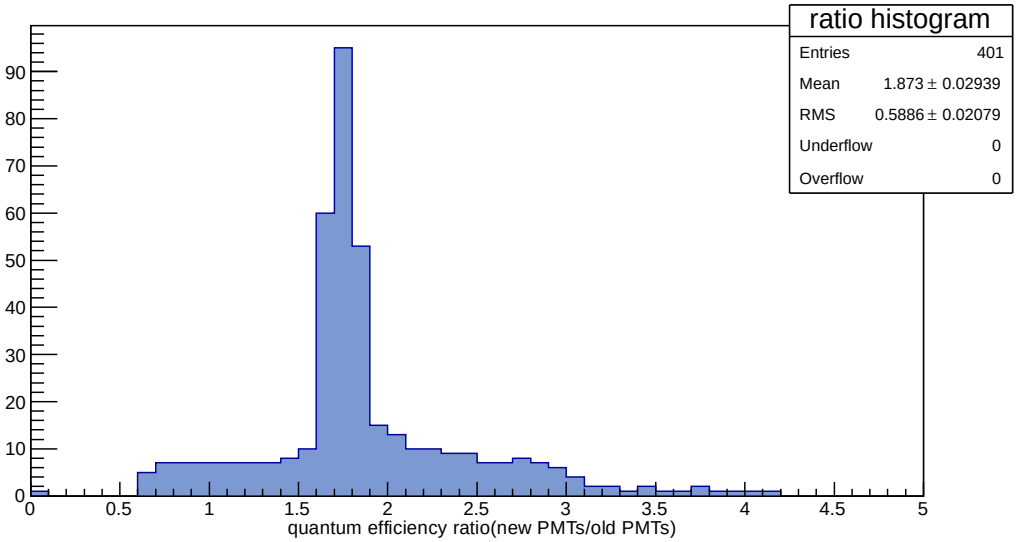

Figure 3.4: Ratio of quantum efficiencies.

New PMT is also more suited to long term use. This is very important HF because it is located in high η values that radiation damage is maximum. New PMT's gain drop is 10% more than old PMT's. Even so in five years of usage, new PMT's quantum efficiency will drop to the old PMT's quantum efficiency and behave like a R7525 model [5].

3.1.3 Implemantation

3.1.3.1 Implemantation in data acquisition

After the signal produced in the quartz fibers, it is directed to the read out boxes with the help of light guides. Readout box houses twenty four PMTs. One anode of PMT is read as one channel. Since new PMTs have four anodes they can be read in different ways. One can join the two anodes of the PMT together and read it out like a 2 anode PMT or all of anodes can be read out separately. This will cause to some modifications on the readout modules. On the other hand one should also change the software to in accord with reading style.

3.1.3.2 Implemantation in CMSSW

For software to produce photoelectrons according to new PMT specifications, quantum efficiency information must be implemented in the CMSSW. The software already creating photo electrons as a function of the the wavelength of the incoming photon.

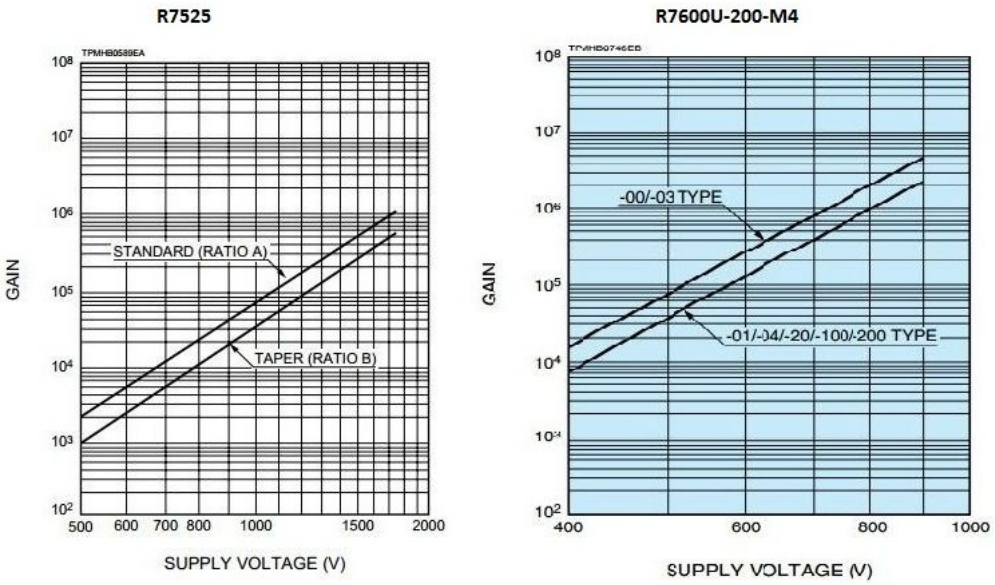

Figure 3.5: Gain difference of old and new PMT [6], [7].

This function is defined and used in Geant 4 simulation of CMS, in the code responsible from producing Cherenkov photons, HFCherenkov.cc. This part of the code simulates the Cherenkov photons and physics process that is related to them.

To change the HFCherenkov.cc accordingly, the quantum efficiency function of new PMTs must be known. However Hamamatsu gives only the PMT's quantum efficiency graphic that shows quantum efficiency versus wavelength. To extract the data points associated with the curve, GetData Graph Digitizer program is used [13]. Using the data points taken, a function is fitted with the help of the data analysis program called ROOT [14]. Then this function is included into the HFCherenkov.cc code similar to the old PMT is. Old PMT's function was not removed from the code, instead, a boolen parameter introduced to easily switch between the parameters of old and new PMT.

3.2 Showers

This section will explain the the electromagnetic and hadronic showers, and the difference between them. It will also explain how they are measured in quartz fiber calorimeters.

3.2.1 Electromagnetic showers

Electrons lose their energy due to ionization and radiation in the absorber. Energy loss by ionization means that while electron passing through the absorber, it interacts

by nearby atoms via processes like Compton scattering and photoelectric effect and give some of its energy to them. These kinds of interaction are dominant in the low energy region. At high energy region above 1 GeV, electrons radiates photons due to bremsstrahlung that will produce showers in the absorber material [8].

Most energetic photons will make pair production and create electron and positron pairs, that again will produce more photons. This way the energy will be quickly deposited. The amount of energy deposited in material is strongly related to the X_0(radiation length) of particle in that particular absorber. Radiation length depends largely on the mass number Z of absorber. It is proportional with $\frac{A}{Z^2}$ where A is atom number [8]. Radiation length says in one X_0 that the particle lose $1-\frac{1}{e}$ of its energy and that length is relatively small for electrons, as it is seen in Figure 3.6. Copper with $Z = 29$ is similar to the HF steel absorber, will capture %90 of the shower energy for 100 GeV electrons in 15 X_0 which will be 21 cm and iron with $Z = 26$ will capture %92 of the shower energy in 15 X_0 which will be 26 cm .

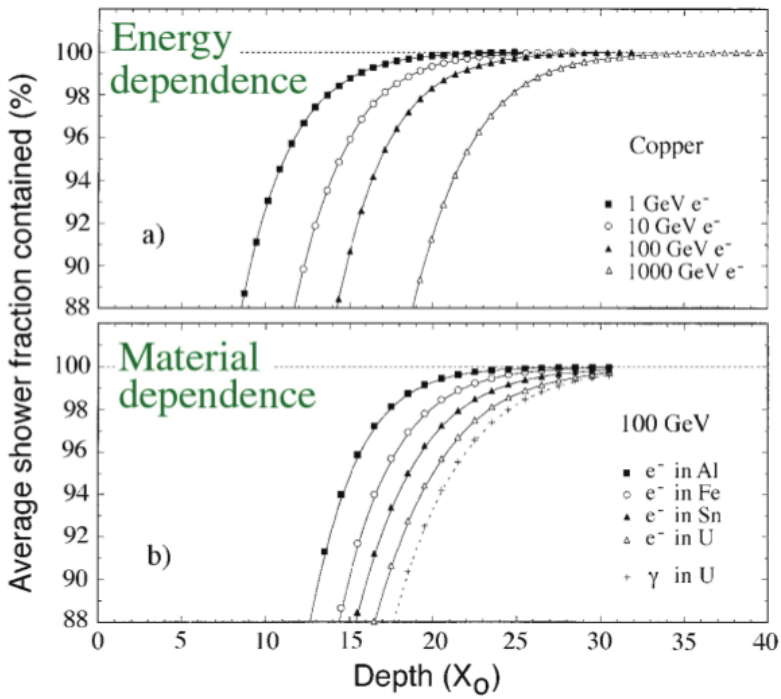

Figure 3.6: Radiation lengths to capture electromagnetic showers in different materials [8].

3.2.2 Hadronic showers

Energy deposition in the hadronic showers is more elaborate than electromagnetic showers due to strong interactions. Nuclear interactions that release the nuclear

binding energy between neutrons and protons gives a signal not detectable by the calorimeters. There is also electromagnetic showers that occurs via the π^0 decaying into 2γ. Without these two effects, energy deposition due to ionization is small in hadronic showers [8].

Similarly like X_0, hadronic showers has λ_{int}(nuclear interaction length) that defines how much will particles travel before they have a nuclear interaction and lose energy. It is proportional with atom number like $\sqrt[3]{A}$ [8]. In comparison with X_0, λ_{int} has much larger value, and because of that hadronic showers start later in the absorber. As a continuation from earlier example, in iron 100 GeV pions lose %92 of their energy in $5\lambda_{int}$ which corresponds to 83 cm as it is seen in Figure 3.7.

Since electromagnetic and hadronic showers have different interaction lengths to deposit their energy, it makes possible to determine the shower type using these properties.

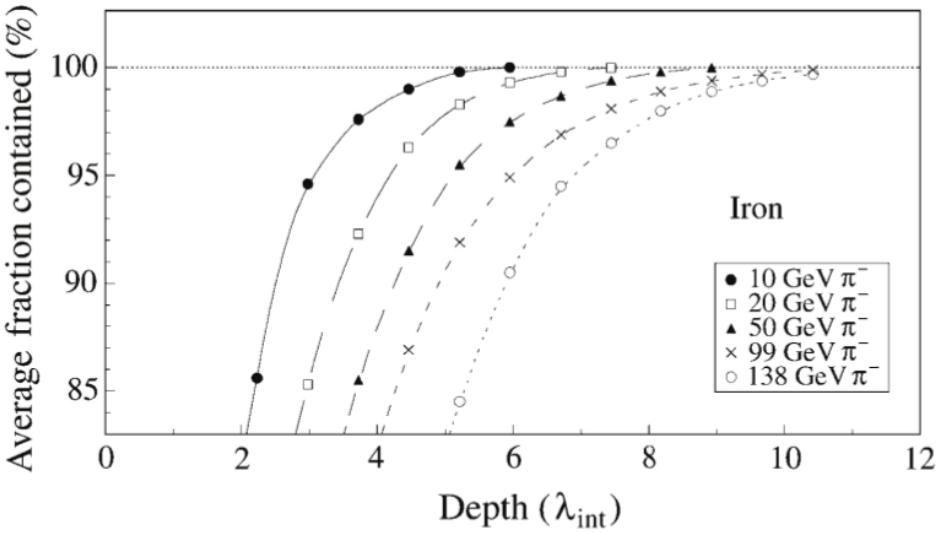

Figure 3.7: Nuclear interaction lengths to capture hadronic showers in iron [8].

3.2.3 Quartz fiber calorimeters

3.2.3.1 Working principle

Quartz fibers detect photons that are produced by Cherenkov radiation. A photon's speed reduced by $\frac{c}{n_{medium}}$ in a different medium than vacuum, where c is the speed of light. However, if a particle's speed is greater then the photon's speed in the medium, Cherenkov photons are released in the shape of a cone. The number of Cherenkov

photons are calculated in Geant 4 with,

$$N_{ph} = \left[2\pi\alpha \left(\frac{1}{\lambda_1} - \frac{1}{\lambda_2} \right) . \sin^2 \theta_C \right] .x \tag{3.1}$$

where N_{ph} is number of Cherenkov photons, α is fine structure constant, λ's are the wavelength interval where Cherenkov photons can be produced, θ is the Cherenkov angle and x is the step length of Geant 4 simulation [9].

The simulation then checks whichever the photons in the Cherenkov cone hit the fiber surface with the appropriate angle so they remain trapped inside the quartz fiber. This process can be understand easier in Figure 3.8.

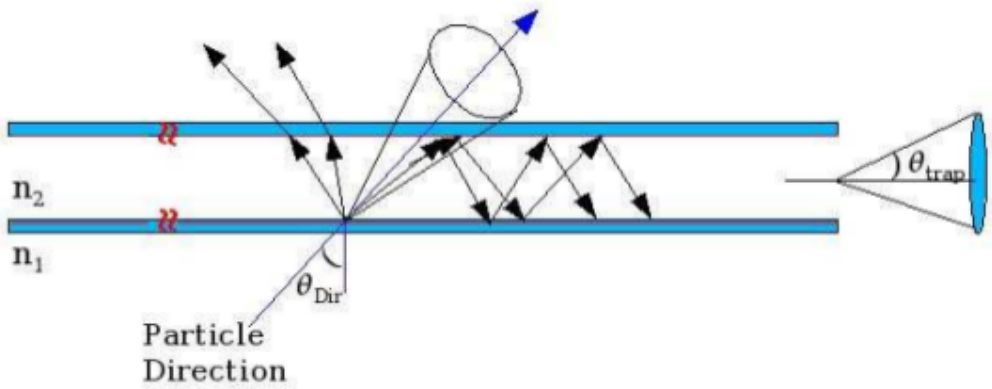

Figure 3.8: Trapping angle of Cherenkov photons [9].

3.2.3.2 Advantages of quartz fiber calorimeters

This kind of Cherenkov light capturing calorimeter have several advantages due to Cherenkov radiation itself. First of all the Cherenkov process is very fast, accomplishing faster event rates than LHC bunch crossing time of 25 ns. Also slow moving particles like neutrons and non relativistic particles can not produce Cherenkov radiation because their speed is essentially lower than the speed of light in the quartz. This property makes detector incapable of detecting these particles reduce the noise. On the other hand, since all of the signal is coming from electrons and positrons, electromagnetic part of hadronic showers becomes dominant at high energies. Since electromagnetic shower's interaction length is much smaller than the hadronic showers, Cherenkov detectors reduce the amount of material to capture hadronic showers [15].

Other advantages of quartz fiber calorimeters comes from the geometry. Since only at a selected angle of particles captured in the fibers, calorimetry also gives information about the trajectories of incoming particles. Width of hadronic showers are also

measured more precise so it can help with jet identification [16]. Quartz fibers also has good radiation tolerance and give good results at high radiation doses [17].

3.3 Simulation of HF PMT

Simulation of the CMS is performed by Geant 4 simulation package. However these kind of detectors have very complex structures and components. To track and simulate a particle through the detector is a CPU demanded process. There is also secondary particles created while a particle simulated. Because all of this, full Geant 4 simulation takes a lot of time. In the case of HF PMTs the important part is the electromagnetic and hadronic showers in HF absorber altough there is much more details in full Geant 4 simulation. To make this HF simulation process faster, there are couple of methods used in CMS software.

3.3.1 HF GFlash

GFlash is a Geant 4 parametrization package that is written to shorten the simulation time of electromagnetic and hadronic showers while preserving quality. GFlash uses a set of equations that have user decided parameters to simulate a shower in the calorimeter in longitudinal direction. Since it simulates a shower, it removes the necessity of tracking all of the secondary particles individually. For the parametrization of shower in the longitidunal direction, GFlash uses a gamma distribution. It assumes the the detector is ϕ independent [18].

When considered to use GFlash in barrel region of CMS, parametrization of shower become difficult due to the different layers of calorimetry, since particles will interact along their way to the HB. On the other hand HF detector is more suitable for GFlash because it does not have any additional layer of calorimeter in front of it. It is also a faster method than full Geant 4 simulation and have good comparability for it. However GFlash must be tuned according to changes in the detector structure. In the case of PMT change, one must know which particles do what kind of showers due to PMT specifications and that is not possible without the information from a full simulation on the HF showers. Without shower library information or from full HF Geant 4 simulation, GFlash can not be tuned.

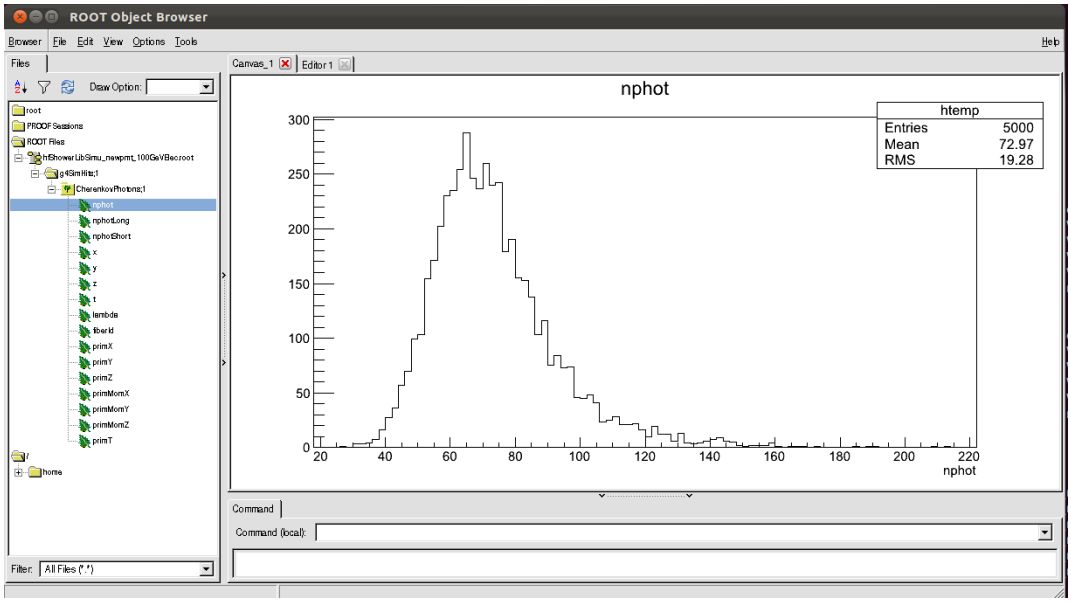

Figure 3.9: Histogram of the number of photoelectrons produced in PMT by 100 GeV electrons, stored in the simulation ROOT file.

3.3.2 Shower Library

HF Shower Library is also a method for simulating PMTs in a more faster way. Main idea is to make a library that contains the information about photons produced in response to the showers, so this information can be extracted and used without the need of a full PMT simulation.

Setting up the correct parameters enable the usage of Shower Library in simulation. When a particle comes to the psuedorapidity region for HF, instead of a full simulation, HF Shower Library is activated. According to the energy and type of particle, corresponding generated photon values in PMT are taken from the chosen Shower Library. With Shower Library for each type of PMT, one can easily change its simulation without worrying about changing the software.

3.3.2.1 Constructing Shower Library

To produce Shower Library a Geant 4 simulation is made for electromagnetic and hadronic showers. For electromagnetic showers electrons are used and for the hadronic showers pions are used with the random transverse η plane gun producer defined in CMS software. The particles are directed to a point in PMT and the resulted shower information is collected at ROOT files for each energy. These ROOT files have the information about how many photons are produced both in long and short fibers, their positions, wavelengths, time informations and more as it is seen in Figure 3.9.

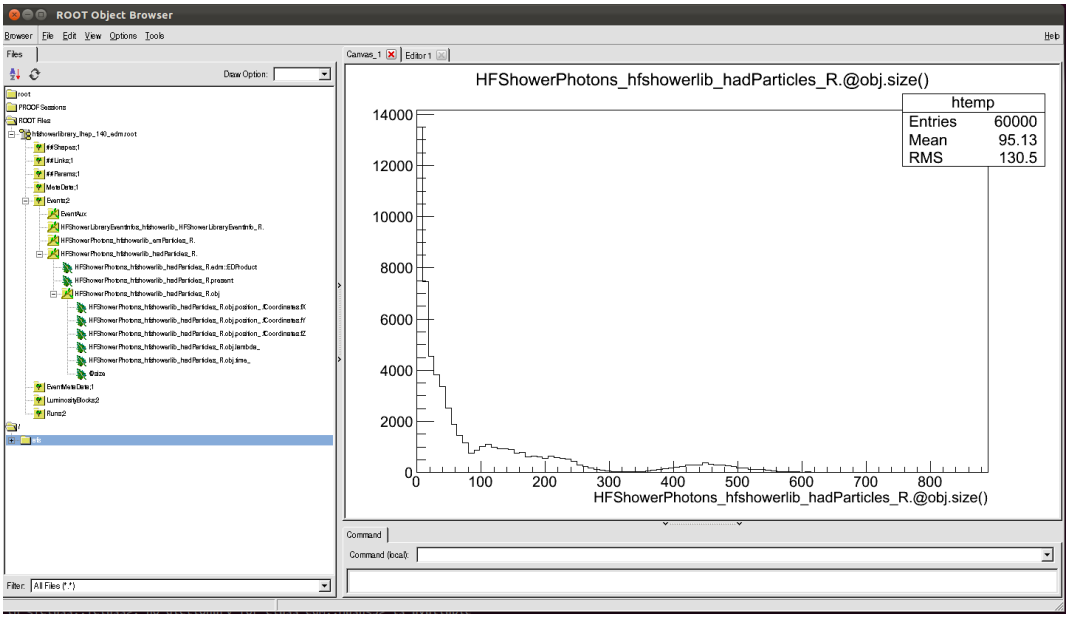

Figure 3.10: Old Shower Library ROOT structure and the histogram of the number of photoelectrons produced in PMT for all energies.

Since all of this simulation takes a lot of time and CPU, the Geant 4 simulation is made over the CMS batch mode, meaning the simulation job is divided into parts and run on different computers connected to the CMS batch job system. Still these produced ROOT files needed to be put in the Shower Library and with the right format used by older Shower Library. To achieve this a Shower Library writer program is written. The writer read all the ROOT files from a list and produced the Shower Library.

3.3.2.2 Old and new Shower Library

There is already a written Shower Library for the old PMTs that have lower quantum efficiencies. This library consist of twelve different energy bins for two different type of showers, electromagnetic and hadronic. For each of the shower type following information is available in the library (Figure 3.10):

- x, y, z position
- wavelength
- time
- number of photo-electrons

For each energy bin there are 5000 events.

The physics list used to produce these events LHEP was chosen because it was the best one to explain the test beam data taken [9]. It is a physics list best to use in parametrized models in high energy physics usually for shower modeling. It includes standard Geant 4 electromagnetic interactions like pair production, photo electric effect and Thompson scattering. For leptons it has multiple scattering, ionization, bremsstrahlung, annihilation and pair production effects and for hadrons it has multiple scattering, ionization and inelastic collisions. LHEP also contain photo-nuclear interactions.

When creating the Shower Library for the new PMTs, same structure is constructed to maintain compatibility. Same number of events at same conditions are simulated for new PMTs with the new software. However to confirm the credibility of new Shower Library, an another Shower Library containing old PMTs is prepared to compare with the already written old Shower Library.

Physics list again chosen to be similar. LHEP-EMV is a list that gave same results with LHEP, only it has a different parametrization of electromagnetic process for a faster simulation that does not lose precision much.

4. RESULTS AND CONCLUSIONS

In this chapter the results of the old and the new PMT's simulations will be given and discussed.

4.1 Results of HF Shower Library

4.1.1 Old Shower Library

Before going into the simulation of new PMT, Shower Library for the older PMT was reconstructed. Similar to the already produced Shower Library for the old PMT, simulations made at twelve energy bins 10 GeV, 15 GeV, 20 GeV, 35 GeV, 50 GeV, 80 GeV, 100 GeV, 150 GeV, 250 GeV, 350 GeV, 500 GeV and 1000 GeV. For hadronic showers pions are used in the simulation and for electromagnetic showers electrons are used. In the simulation GFlash, parametrization of showers, PMT window hits and other additional effects are excluded. 5000 events are generated for each energy and each shower type.

For 100 GeV electrons simulation of the photo-electrons produced in long fiber is shown in Figure A.1(a) and in short fiber is seen in Figure A.1(b). Same simulation for 100 GeV pions is seen in Figure A.2(a) and Figure A.2(b).

Between the existing Shower Library results and newly produced old Shower Library there is a good compatibility. The difference comes from how the Geant 4 simulation is made, however, mostly it comes from the statistical fluctuations. It can be shown that statistical errors are reduced by increasing the event number. Since there is no existing data that have more than 5000 events, a comparison made by producing two sets of same simulation with higher event number by changing the initial random number seeds. 50000 events are produced in Figure A.3(a) and Figure A.3(b) for photo-electrons produced in long fiber and short fiber for 100 GeV electrons.

Table 4.1: Comparison of simulation with 5000 and 50000 events in Long fiber.

Electromagnetic Shower 100 GeV Electrons Long fiber	Mean-RMS
Old Shower Library(5000 events)	32.98±0.15 - 10.61±0.10
Produced old Shower Library(50000 events)	32.67±0.05 - 10.40±0.03
Produced old Shower Library(50000 events)	32.76±0.05 - 10.30±0.03

Table 4.2: Comparison of simulation with 5000 and 50000 events in Short fiber.

Electromagnetic Shower 100 GeV Electrons Short fiber	Mean-RMS
Old Shower Library(5000 events)	8.11±0.07 - 4.68±0.05
Produced old Shower Library(50000 events)	7.89±0.02 - 4.69±0.01
Produced old Shower Library(50000 events)	7.89±0.02 - 4.69±0.01

Comparison between Figure A.1 and Figure A.3 shows that with greater number of events the ratio of two curve come closer to the one. As it is seen in the Table 4.1 and Table 4.2, the deviation of the mean and RMS are reduced. Since the errors reduce with the square root of event number, one must produce at least $15^2.5000 = 1250000$ events to reduce 15% error in the long fiber in Table 4.1 to 1%.

For a final confirmation, for all energy bins, the ratio of mean's and RMS's of existing and produced old Shower Library was plotted subsequently in Figure A.4 and Figure A.5. The detailed information about the old Shower Libraries can be found in the Table A.1 and Table A.2.

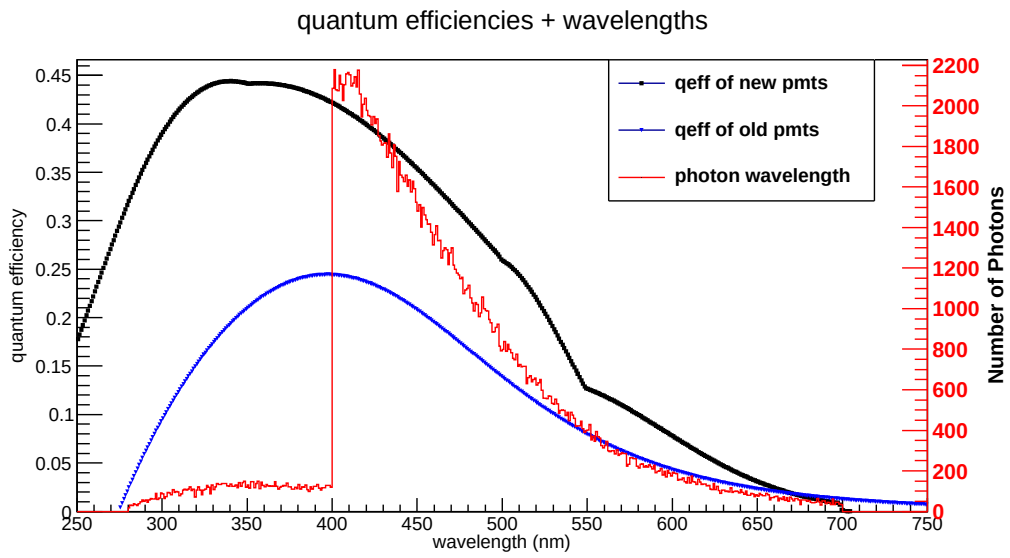

Figure 4.1: Quantum efficiency difference of old and new PMT.

4.1.2 New Shower Library

For producing the Shower Library for the new PMTs a function defines the quantum efficiency of new PMT was written. This function can be found in Appendix B. When quantum efficiency of new PMT is plotted against the quantum efficiency of old PMT and the accident photons wavelengths, it is seen in Figure 4.1 that quantum efficiency of new PMT is higher. It is also evident that peak of the new PMT's quantum efficiency is not aligned like the peak of old PMT with the wavelengths of photons.

Simulations are made in the same energy bins and at same event number as old Shower Library. Since new PMT's have 1.8 times higher quantum efficiency than old PMT, observation of higher number of photo-electrons is expected. This behavior confirmed and evident in Figure A.6 and Figure A.7 for both electrons and pions at 100 GeV. This difference is also existing in the other energy bins. A round up of comparison for old and new PMT for all energies is in Table A.3 and Table A.4.

4.2 Conclusion

In conclusion, a new Shower Library for the newest CMSSW version was created. The method used gave good results in comparison with the existing Shower Library. Expectation of a higher count of photo-electrons due to the quantum efficiency of the new PMTs has been observed. The results indicated also a higher RMS for the new PMTs. It should be also noted that the wavelength of incoming photons was tuned in accord with the old PMTs quantum efficiency function. Since the new PMTs have different peak value for their quantum efficiencies, wavelengths of Cherenkov photons must be set in accord with in newer simulations.

The benefits of using the new PMTs and the new Shower Library can be observed in physics processes, where sensitivity is important. This will be the future aim of this study.

REFERENCES

[1] **Blanchet, L.**, **Spallicci, A. and Whiting, B.**, (2011). Mass and Motion in General Relativity, Springer.

[2] **CERN Website**. <http://public.web.cern.ch/public/en/lhc/CMS-en.html>, Accessed: 01.05.2012.

[3] **Breskin, A. and Voss, R.**, (2009). The CERN Large Hadron Collider: Accelerator and Experiments Volume 2: CMS LHCb, LHCf and TOTEM, The Scientific Information Service CERN.

[4] **CMS Collaboration**, (2006). CMS Physics Technical Design Report Volume 1: Detector Performance and Software, The Scientific Information Service CERN.

[5] **Yetkin, T. and Önel, Y.**, (2010), Candidate PMT: Specs and Radiation Studies, CMS HCAL HF PMT replacement ECR.

[6] **Hamamatsu**, Photomultiplier Tube R7525 Datasheet.

[7] **Hamamatsu**, Photomultiplier Tube R7600U Series Datasheet.

[8] **Wigmans, R.**, (2008). Calorimetry, *Scientifica Acta*, **2(1)**, 18 – 55.

[9] **Yetkin, T. and Kunori, S.**, (2006). GEANT4 Simulation of the CMS Forward Calorimeter in the 2004 Test Beam, *CMS IN*, **2006/018**.

[10] **Breskin, A. and Voss, R.**, (2009). The CERN Large Hadron Collider: Accelerator and Experiments Volume 1: LHC Machine, ALICE and ATLAS, The Scientific Information Service CERN.

[11] **CMS Collaboration**, (2006). CMS physics Technical Design Report, Volume II: Physics Performance, The Scientific Information Service CERN.

[12] **Bilki, B. et al.**, (2010). Study of various photomultiplier tubes with muon beams and Cherenkov light produced in electron showers, *2010 JINST 5 P06002*.

[13] **Getdata Graph Digitizer**. <http://www.getdata-graph-digitizer.com/>, Accessed: 02.05.2012.

[14] **ROOT Website**. <http://root.cern.ch/>, Accessed: 02.05.2012.

[15] **N. Akchurin et al.**, (1997). Beam test results from a fine-sampling quartz fiber calorimeter for electron, photon and hadron detection, *Nuclear Instruments and Methods in Physics Research A*, **399**, 202 – 226.

[16] **Önel, Y. and Penzo, A.**, (2008). The CMS-HF quartz fiber calorimeters, *Journal of Physics: Conference Series*, **160**.

[17] **Merlo, J.P. and Cankocak, K.**, (2006). Radiation Hardness Studies of high OH-Content Quartz Fibers Irradiated with 24 GeV Protons, *CMS CR*, **2006/005**.

[18] **Geant 4**, (2011), Physics Referance Manual.

[19] **ROOT Website - TMath**. <http://root.cern.ch/root/html/TMath.html:TMath:Landau>, Accessed: 01.05.2012.

APPENDICES

APPENDIX A : Results Of Old Shower Library And New Shower Library Data
APPENDIX B : Function Of New PMT's Quantum Efficiency

APPENDIX A

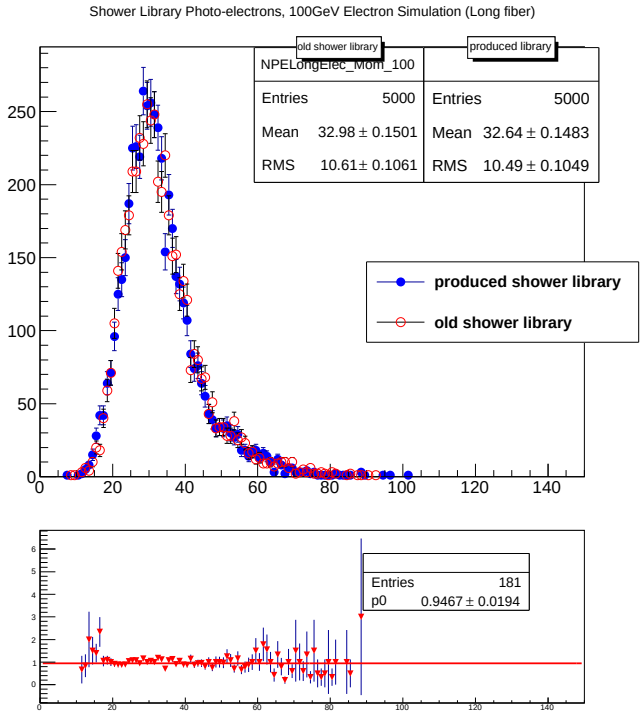

(a) Long fiber

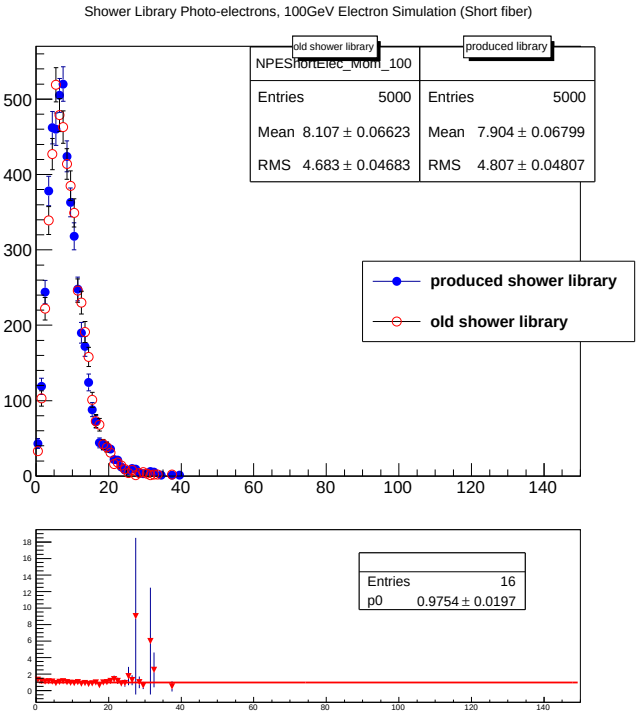

(b) Short fiber

Figure A.1: Comparison of photo-electrons produced in electron simulation between existing old Shower Library and newly produced old Shower Library : Long fiber (a). Short fiber (b).

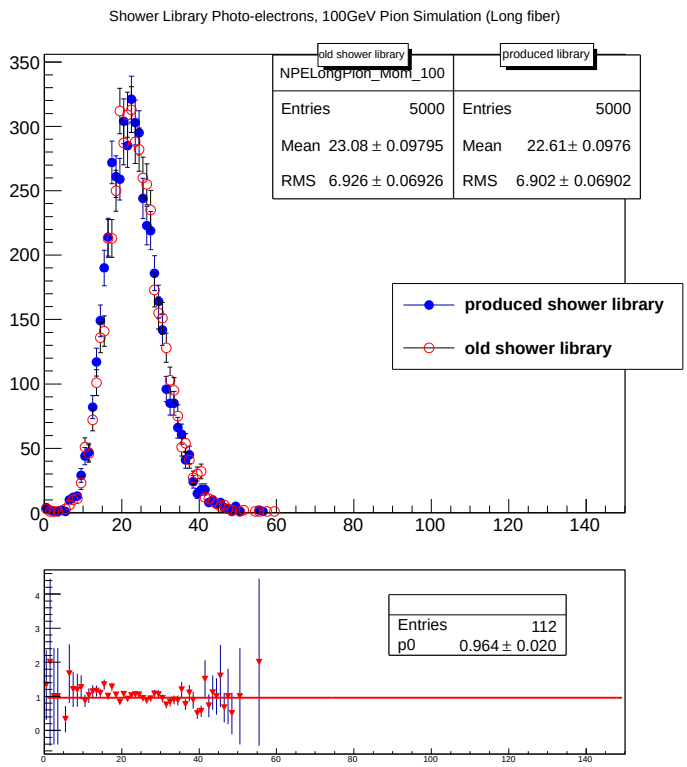

(a) Longfiber

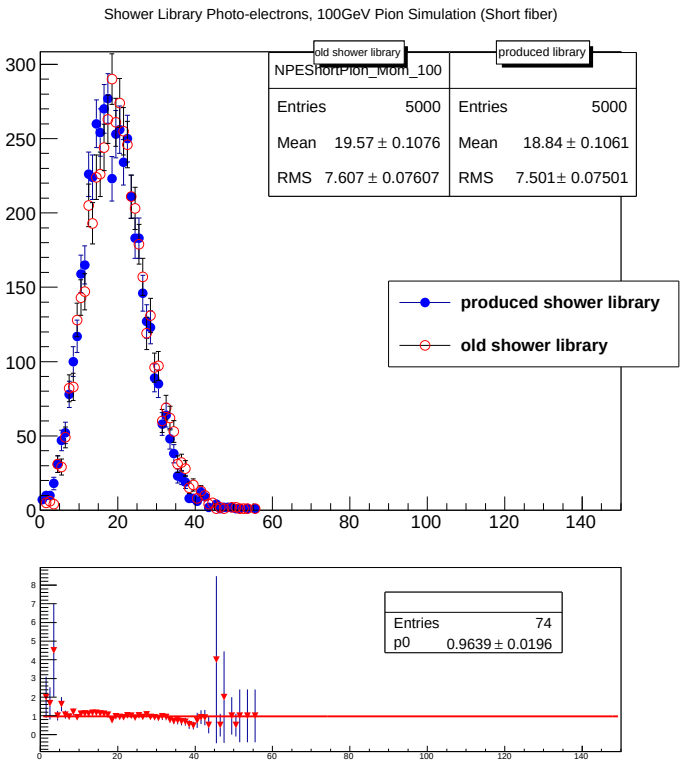

(b) Shortfiber

Figure A.2: Comparison of photo-electrons produced in pion simulation for existing old Shower Library and newly produced old Shower Library : Long fiber (a). Short fiber (b).

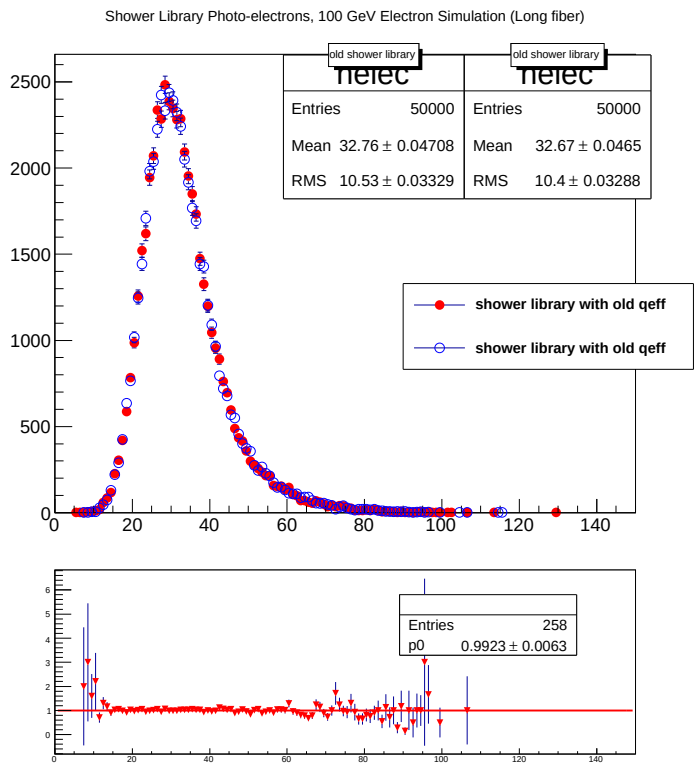

(a) Long fiber

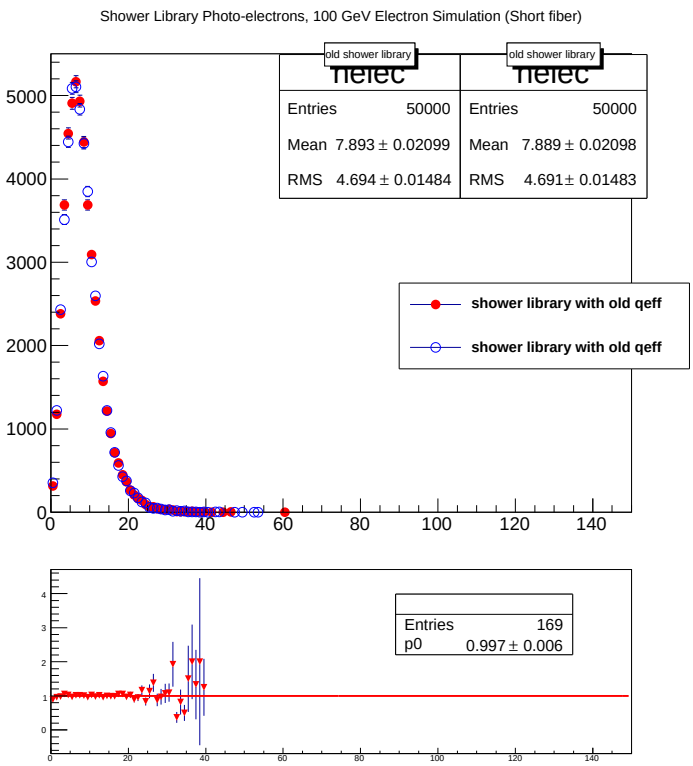

(b) Short fiber

Figure A.3: Comparison of photo-electrons produced in electron simulation for two sets of newly produced data with 50000 events : Long fiber (a). Short fiber (b).

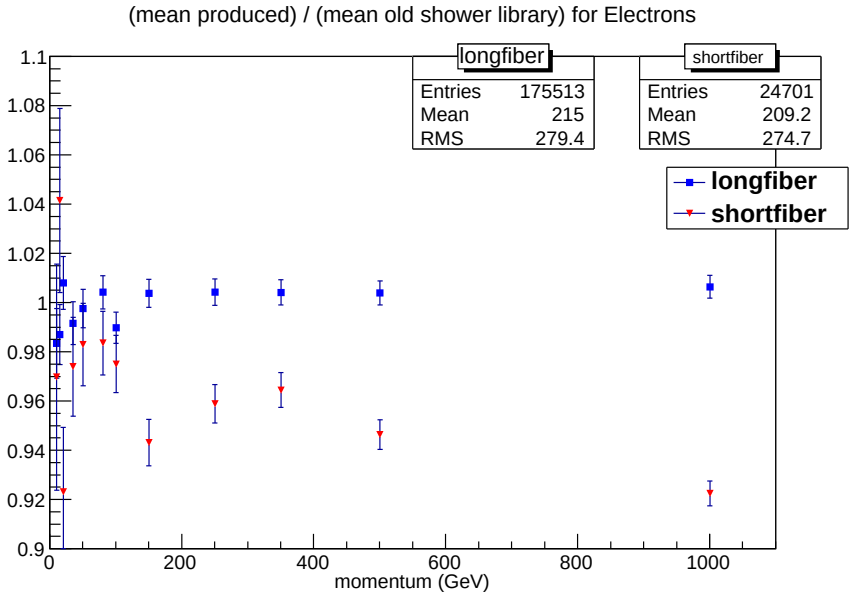

(a) Electrons

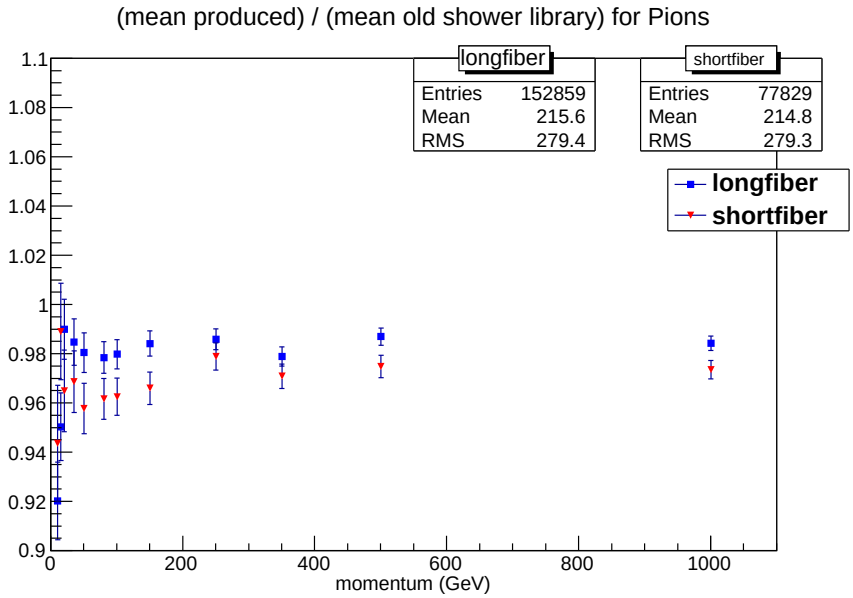

(b) Pions

Figure A.4: Ratio of produced photo-electrons means's for each energy bin: For electrons (a). For pions (b).

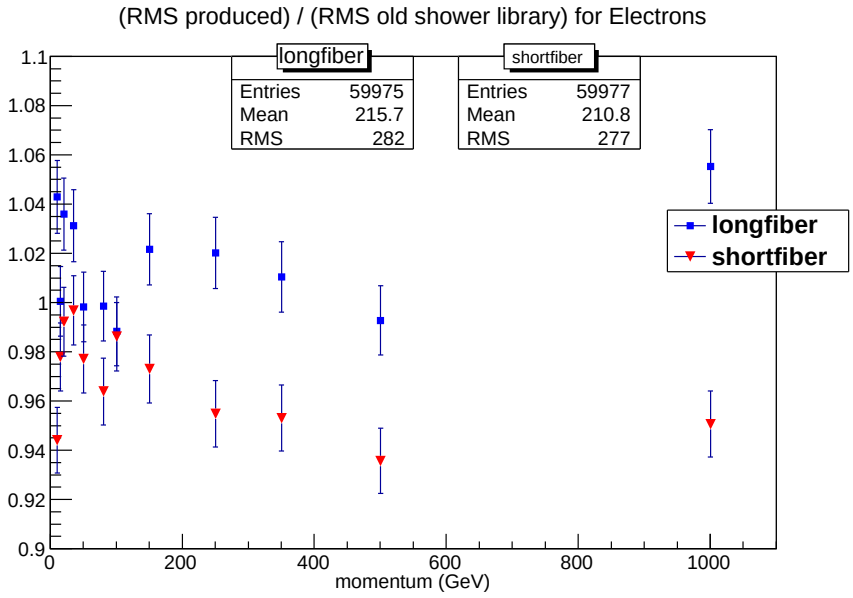

(a) Electrons

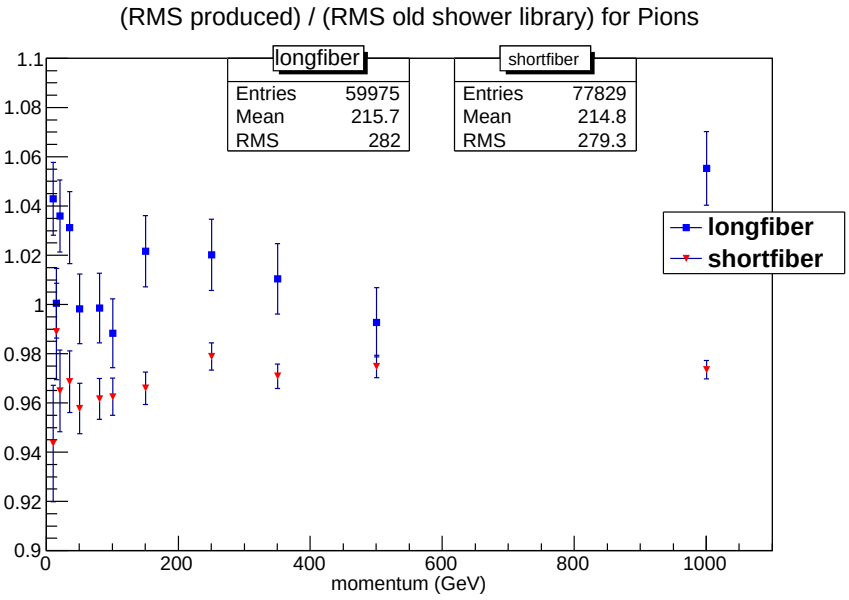

(b) Pions

Figure A.5: Ratio of produced photo-electrons RMS's for each energy bin: For electrons (a). For pions (b).

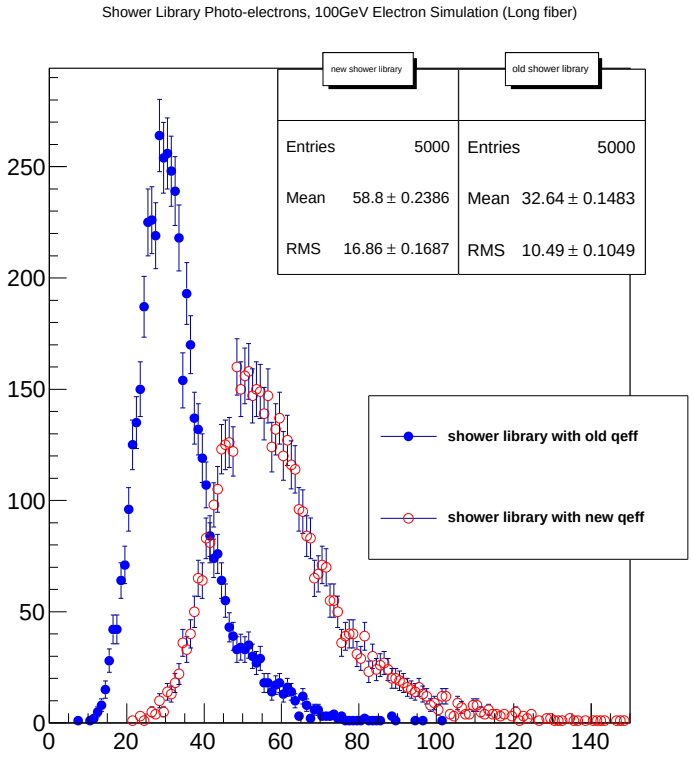

(a) Long fiber

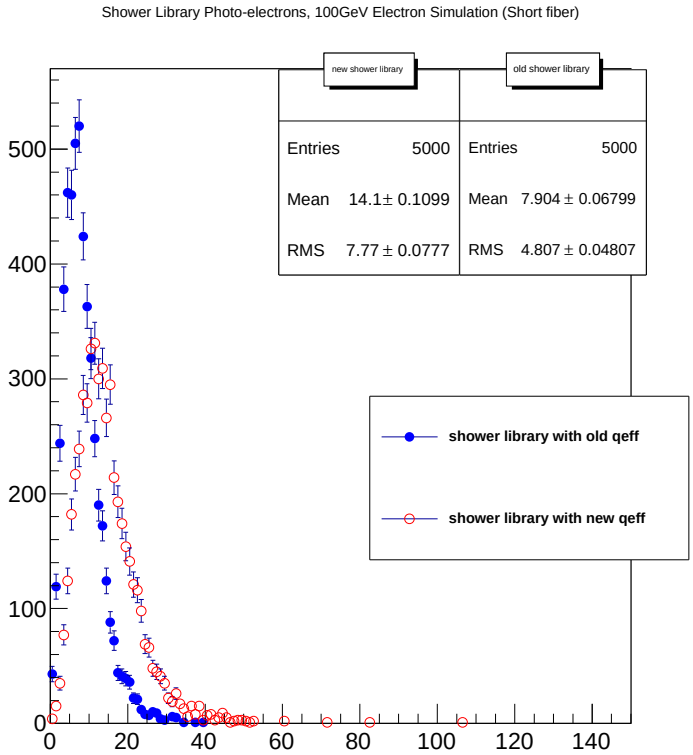

(b) Short fiber

Figure A.6: Comparison of photo-electrons produced in electron simulation for old and new Shower Library: Long fiber (a). Short fiber (b).

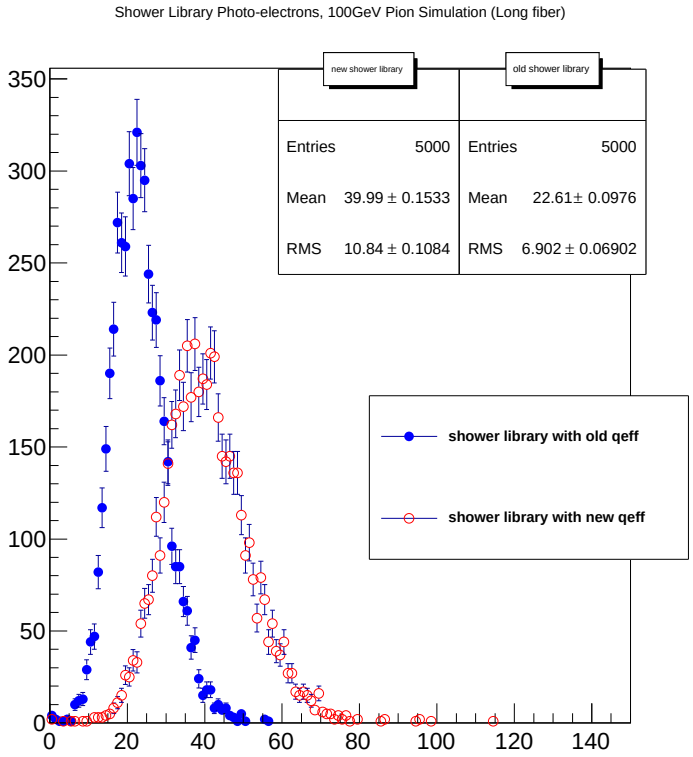

(a) Long fiber

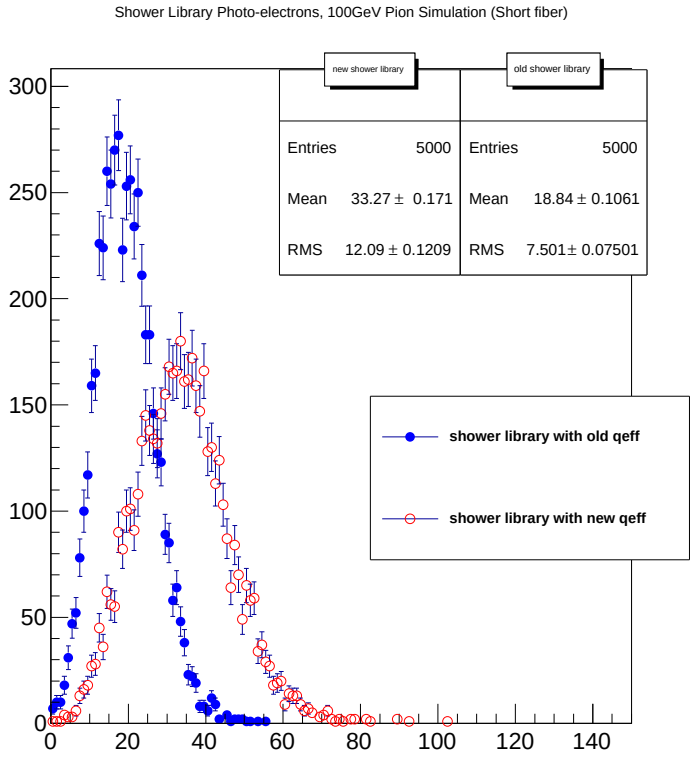

(b) Short fiber

Figure A.7: Comparison of photo-electrons produced in pion simulation for old and new Shower Library: Long fiber (a). Short fiber (b).

Table A.1: Mean and RMS of number of photon-electrons produced by electrons

Electromagnetic Shower Longfiber						
Energy of Electron	10 GeV	15 GeV	20 GeV	35 GeV	50 GeV	80 GeV
	Mean-RMS	Mean-RMS	Mean-RMS	Mean-RMS	Mean-RMS	Mean-RMS
Old-old Shower Library	3.29±	4.96±0.04	6.44±0.04	11.50±0.06	16.39±0.09	26.19±0.12
	2.30±	3.05±0.03	3.38±0.03	4.95±0.04	6.39±0.06	8.82±0.08
New-old Shower Library	3.24±	4.89±0.04	6.49±0.04	11.40±0.07	16.35±0.09	26.30±0.12
	2.40±	3.04±0.03	3.50±0.03	5.10±0.05	6.38±0.06	8.81±0.08
Energy of Electron	100 GeV	150 GeV	250 GeV	350 GeV	500 GeV	1000 GeV
	Mean-RMS	Mean-RMS	Mean-RMS	Mean-RMS	Mean-RMS	Mean-RMS
Old-old Shower Library	32.98±0.15	48.91±0.19	81.60±0.30	114.40±0.40	163.40±0.56	325.50±1.02
	10.61±0.10	13.84±0.13	21.57±0.21	28.66±0.28	40.21±0.40	72.44±0.72
New-old Shower Library	32.64±0.14	49.09±0.20	81.95±0.31	114.80±0.40	164.00±0.56	327.6±1.08
	10.49±0.10	14.14±0.14	22.00±0.22	28.96±0.28	39.92±0.39	76.45±0.76
Shortfiber						
Energy of Electron	10 GeV	15 GeV	20 GeV	35 GeV	50 GeV	80 GeV
	Mean-RMS	Mean-RMS	Mean-RMS	Mean-RMS	Mean-RMS	Mean-RMS
Old-old Shower Library	0.34±0.01	0.59±0.01	0.93±0.02	2.03±0.03	3.19±0.04	5.97±0.05
	0.78±0.00	1.02±0.01	1.29±0.01	2.09±0.02	2.71±0.03	3.91±0.04
New-old Shower Library	0.33±0.01	0.61±0.01	0.85±0.02	1.97±0.03	3.14±0.04	8.87±0.05
	0.81±0.00	1.13±0.01	1.24±0.01	2.02±0.02	2.69±0.03	3.89±0.04
Energy of Electron	100 GeV	150 GeV	250 GeV	350 GeV	500 GeV	1000 GeV
	Mean-RMS	Mean-RMS	Mean-RMS	Mean-RMS	Mean-RMS	Mean-RMS
Old-old Shower Library	8.11±0.07	14.00±0.10	26.97±0.16	40.92±0.21	65.04±0.29	156.10±0.62
	4.68±0.05	7.08±0.07	11.17±0.11	14.88±0.15	20.83±0.21	44.11±0.44
New-old Shower Library	7.90±0.07	13.20±0.09	25.86±0.15	39.47±0.21	61.55±0.27	144.00±0.54
	4.81±0.05	6.56±0.06	10.39±0.10	14.57±0.15	19.50±0.19	38.31±0.38

Table A.2: Mean and RMS of number of photon-electrons produced by pions

Hadronic Shower Longfiber						
Energy of Pion	10 GeV	15 GeV	20 GeV	35 GeV	50 GeV	80 GeV
	Mean-RMS	Mean-RMS	Mean-RMS	Mean-RMS	Mean-RMS	Mean-RMS
Old-old Shower Library	2.11±0.02	3.26±0.03	4.24±0.04	7.61±0.05	11.19±0.06	18.26±0.08
	1.72±0.02	2.29±0.02	2.57±0.02	3.66±0.04	4.54±0.04	5.98±0.06
New-old Shower Library	1.94±0.02	3.09±0.03	4.12±0.04	7.49±0.05	10.97±0.06	17.87±0.08
	1.74±0.02	2.29±0.02	2.62±0.03	3.61±0.04	4.50±0.04	5.92±0.06
Energy of Pion	100 GeV	150 GeV	250 GeV	350 GeV	500 GeV	1000 GeV
	Mean-RMS	Mean-RMS	Mean-RMS	Mean-RMS	Mean-RMS	Mean-RMS
Old-old Shower Library	23.08±0.10	34.72±0.13	58.57±0.18	83.23±0.52	118.80±0.30	241.20±0.52
	6.93±0.07	8.94±0.09	12.61±0.13	16.23±0.37	20.80±0.21	36.88±0.37
New-old Shower Library	22.61±0.10	34.17±0.13	57.74±0.18	81.47±0.23	117.30±0.29	237.40±0.50
	6.90±0.07	9.00±0.09	12.50±0.12	16.30±0.16	20.38±0.20	34.95±0.35
Shortfiber						
Energy of Pion	10 GeV	15 GeV	20 GeV	35 GeV	50 GeV	80 GeV
	Mean-RMS	Mean-RMS	Mean-RMS	Mean-RMS	Mean-RMS	Mean-RMS
Old-old Shower Library	1.30±0.02	2.09±0.03	3.00±0.03	5.77±0.05	9.02±0.07	15.27±0.09
	1.62±0.02	2.08±0.02	2.54±0.02	3.67±0.04	4.78±0.05	6.58±0.06
New-old Shower Library	1.23±0.02	2.07±0.03	2.90±0.03	5.59±0.05	8.64±0.07	14.68±0.95
	1.53±0.01	2.03±0.02	2.52±0.02	3.66±0.04	4.67±0.05	6.34±0.06
Energy of Pion	100 GeV	150 GeV	250 GeV	350 GeV	500 GeV	1000 GeV
	Mean-RMS	Mean-RMS	Mean-RMS	Mean-RMS	Mean-RMS	Mean-RMS
Old-old Shower Library	19.57±0.11	30.07±0.14	51.15±0.21	73.26±0.27	106.20±0.29	218.50±0.60
	7.61±0.08	10.19±0.10	14.68±0.15	19.11±0.20	25.09±0.21	42.11±0.42
New-old Shower Library	18.4±0.11	29.05±0.14	50.07±0.20	71.13±0.26	103.50±0.33	212.70±0.57
	7.50±0.07	9.92±0.10	14.02±0.14	18.22±0.18	23.48±0.23	40.03±0.40

Table A.3: Comparison of mean and RMS of number of photo-electrons produced by electrons between old and new PMT

Electromagnetic Shower						
Long fiber						
Energy of Electron	10 GeV	15 GeV	20 GeV	35 GeV	50 GeV	80 GeV
	Mean-RMS	Mean-RMS	Mean-RMS	Mean-RMS	Mean-RMS	Mean-RMS
Old Shower Library	3.29±	4.96±0.04	6.44±0.04	11.50±0.06	16.39±0.09	26.19±0.12
	2.30±	3.05±0.03	3.38±0.03	4.95±0.04	6.39±0.06	8.82±0.08
New Shower Library	5.90±0.05	8.86±0.07	11.78±0.08	20.47±0.0	29.20±0.15	46.61±0.20
	3.80±0.04	4.82±0.05	5.76±0.06	8.09±0.05	10.46±0.10	14.46±0.14
Energy of Electron	100 GeV	150 GeV	250 GeV	350 GeV	500 GeV	1000 GeV
	Mean-RMS	Mean-RMS	Mean-RMS	Mean-RMS	Mean-RMS	Mean-RMS
Old Shower Library	32.98±0.15	48.91±0.19	81.60±0.30	114.40±0.40	163.40±0.56	325.50±1.02
	10.61±0.10	13.84±0.13	21.57±0.21	28.66±0.28	40.21±0.40	72.44±0.72
New Shower Library	58.80±0.24	87.15±0.33	145.60±0.50	203.40±0.66	288.20±0.90	576.20±1.68
	16.86±0.17	23.12±0.23	35.45±0.35	46.36±0.46	62.68±0.63	118.10±1.19
Short fiber						
Energy of Electron	10 GeV	15 GeV	20 GeV	35 GeV	50 GeV	80 GeV
	Mean-RMS	Mean-RMS	Mean-RMS	Mean-RMS	Mean-RMS	Mean-RMS
Old Shower Library	0.34±0.01	0.59±0.01	0.93±0.02	2.03±0.03	3.19±0.04	5.97±0.05
	0.78±0.00	1.02±0.01	1.29±0.01	2.09±0.02	2.71±0.03	3.91±0.04
New Shower Library	0.60±0.02	1.03±0.02	1.58±0.03	3.46±0.04	5.63±0.06	10.50±0.09
	1.21±0.01	1.62±0.02	2.06±0.02	3.18±0.03	4.33±0.04	6.37±0.06
Energy of Electron	100 GeV	150 GeV	250 GeV	350 GeV	500 GeV	1000 GeV
	Mean-RMS	Mean-RMS	Mean-RMS	Mean-RMS	Mean-RMS	Mean-RMS
Old Shower Library	8.11±0.07	14.00±0.10	26.97±0.16	40.92±0.21	65.04±0.29	156.10±0.62
	4.68±0.05	7.08±0.07	11.17±0.11	14.88±0.15	20.83±0.21	44.11±0.44
New Shower Library	14.10±0.11	24.03±0.16	45.86±0.25	69.91±0.34	110.90±0.49	258.40±0.96
	7.71±0.07	11.24±0.11	18.00±0.18	24.00±0.24	34.47±0.34	68.07±0.68

Table A.4: Comparison of mean and RMS of number of photo-electrons produced by pions between old and new PMT

Hadronic Shower Long fiber						
Energy of Pion	10 GeV Mean-RMS	15 GeV Mean-RMS	20 GeV Mean-RMS	35 GeV Mean-RMS	50 GeV Mean-RMS	80 GeV Mean-RMS
Old Shower Library	2.11±0.02	3.26±0.03	4.24±0.04	7.61±0.05	11.19±0.06	18.26±0.08
	1.72±0.02	2.29±0.02	2.57±0.02	3.66±0.04	4.54±0.04	5.98±0.06
New Shower Library	3.53±0.04	5.53±0.05	7.40±0.06	13.51±0.08	19.59±0.10	31.85±0.13
	2.77±0.03	3.48±0.03	3.99±0.04	5.62±0.06	7.13±0.07	9.67±0.10
Energy of Pion	100 GeV Mean-RMS	150 GeV Mean-RMS	250 GeV Mean-RMS	350 GeV Mean-RMS	500 GeV Mean-RMS	1000 GeV Mean-RMS
Old-old Shower Library	23.08±0.10	34.72±0.13	58.57±0.18	83.23±0.52	118.80±0.30	241.20±0.52
	6.93±0.07	8.94±0.09	12.61±0.13	16.23±0.37	20.80±0.21	36.88±0.37
New Shower Library	39.99±0.15	61.52±0.21	103.40±0.29	145.20±0.36	209.50±0.47	426.10±0.84
	10.84±0.11	14.67±0.15	20.74±0.21	29.59±0.25	33.62±0.34	59.73±0.60
Short fiber						
Energy of Pion	10 GeV Mean-RMS	15 GeV Mean-RMS	20 GeV Mean-RMS	35 GeV Mean-RMS	50 GeV Mean-RMS	80 GeV Mean-RMS
Old Shower Library	1.30±0.02	2.09±0.03	3.00±0.03	5.77±0.05	9.02±0.07	15.27±0.09
	1.62±0.02	2.08±0.02	2.54±0.02	3.67±0.04	4.78±0.05	6.58±0.06
New Shower Library	2.18±0.03	3.66±0.05	5.06±0.05	10.13±0.08	15.47±0.11	26.59±0.15
	2.45±0.02	3.32±0.03	3.94±0.04	5.94±0.06	7.63±0.08	10.53±0.10
Energy of Pion	100 GeV Mean-RMS	150 GeV Mean-RMS	250 GeV Mean-RMS	350 GeV Mean-RMS	500 GeV Mean-RMS	1000 GeV Mean-RMS
Old Shower Library	19.57±0.11	30.07±0.14	51.15±0.21	73.26±0.27	106.20±0.29	218.50±0.60
	7.61±0.08	10.19±0.10	14.68±0.15	19.11±0.20	25.09±0.21	42.11±0.42
New Shower Library	33.27±0.17	51.94±0.23	89.08±0.33	127.00±0.43	184.70±0.55	382.10±0.10
	12.09±0.12	16.63±0.17	23.59±0.23	30.27±0.30	39.26±0.40	69.65±0.70

APPENDIX B

To calculate Q(quantum efficiency), below function is written with λ being wavelength, while $\lambda \leq 350nm$,

$$Q = 2.45867 \times Landau(\lambda, 353.820, 59.1324) \tag{A.1}$$

while $350 < \lambda \leq 500nm$,

$$Q = 0.441989 \exp \frac{-(\lambda - 358.371)^2}{2 \times (138.277)^2} \tag{A.2}$$

while $500 < \lambda \leq 550nm$,

$$Q = 0.271862 \exp \frac{-(\lambda - 491.505)^2}{2 \times (47.0418)^2} \tag{A.3}$$

while $550 < \lambda \leq 700nm$,

$$Q = 0.137297 \exp \frac{-(\lambda - 520.260)^2}{2 \times (75.5023)^2} \tag{A.4}$$

where the definition of *Landau* function in ROOT can be found at their website [19].

CURRICULUM VITAE

Name Surname: Mete Yücel

E-Mail: yucelmet@itu.edu.tr

B.Sc.: Istanbul Technical University Physics Engineering Programme 2010

M.Sc.: Istanbul Technical University Physics Engineering Programme 2012